University of Southern Queensland

School of Civil Engineering and Surveying

Exploring the Application of Closed Form Solutions in Geotechnical Problems

A dissertation submitted by

Timothy Eaton

in fulfilment of

ENG4112 Research Project

towards the degree of

Bachelor of Civil Engineering

Submitted: 17th October, 2013

Supervisor: Kazem Ghabraie

Abstract

This project explores the uses, values and limitations of closed form solutions in specific areas of geotechnical engineering. Three closed form (analytical) solutions, Kelvin's, Boussinesq's and Mindlin's solutions have been chosen and researched to determine their applications in geotechnical engineering. These applications have been examined with the aim to modify, further define and/or extend upon them so that they may be applicable to new problems.

A review of research on Kelvin's, Mindlin's and Boussinesq's solutions gave an indication of the ways each of the solutions could be applied to solve for certain problems. After noting the likeness of the solutions and the accomplishments that had been achieved with the relatively popular Boussinesq's soultion, the aim was to subject the lesser known and utilised Mindlin's solution to similar concepts.

The integration of Mindlin's solution for a sub-surface circular loading was performed and is shown here in full, something which does not appear to have been published. From this Newmark inspired Mindlin based influence charts were generated which were found to be of little practical use. Following this the relationship between both Boussinesq's and Mindlin's solutions was investigated and analysed resulting in the production of a design chart that may be applicable to a bi-loaded anchor system.

On a whole the work undertaken in this dissertation showed the main values of the closed form solution in the area of stresses in soil masses were that of insight and flexibility, and their main limitation was that of the simplifying assumptions that were required to be made.

University of Southern Queensland

Faculty of Health, Engineering and Sciences

ENG4111/2 *Research Project*

Limitations of Use

The Council of the University of Southern Queensland, its Faculty of Health, Engineering Sciences, and the staff of the University of Southern Queensland, do not accept any responsibility for the truth, accuracy or completeness of material contained within or associated with this dissertation.

Persons using all or any part of this material do so at their own risk, and not at the risk of the Council of the University of Southern Queensland, its Faculty of Health, Engineering Sciences or the staff of the University of Southern Queensland.

This dissertation reports an educational exercise and has no purpose or validity beyond this exercise. The sole purpose of the course pair entitled "Research Project" is to contribute to the overall education within the student's chosen degree program. This document, the associated hardware, software, drawings, and other material set out in the associated appendices should not be used for any other purpose: if they are so used, it is entirely at the risk of the user.

Dean

Faculty of Health, Engineering Sciences

Certification of Dissertation

I certify that the ideas, designs and experimental work, results, analyses and conclusions set out in this dissertation are entirely my own effort, except where otherwise indicated and acknowledged.

I further certify that the work is original and has not been previously submitted for assessment in any other course or institution, except where specifically stated.

Student Name: Timothy Eaton
Student Number: 0061004795

Signature: _____

Date: _____

Acknowledgements

A pass of sincere thanks is due to my supervisor, Dr. Kazem Ghabraie. For it was his direction, ideas and willingness to help at all times that gave this thesis its proper flow and structure. I would also like to thank him for providing me with a topic of which I found very interesting, and one that introduced me to the academic process in an exciting manner. Additionally a devout thanks for his assistance in MATLAB and LaTeX coding, two things of which I did not have a high degree of competency with by any means.

Acknowledgement also goes out to my girlfriend, Kirsty, for her support and encouragement. Additional thanks goes out to my family and friends for injecting positivity during the time spent working on this dissertation.

Contents

List of Figures

Chapter 1

Introduction

1.1 Types of Solutions

Before we start, it is worth defining what exactly a *closed form solution* is. An exact definition is a debated topic by mathematicians but for this thesis a solution is of closed-form if an **exact** and nicely *closed* solution can be obtained from a small number of equations, something which could practically be undertaken by hand. Solutions of closed form are also referred to as *analytical solutions*, given that the problem is solved through analysis (Neumann 2004).

Other types of common solutions are numerical solutions and experimental solutions. Numerical solutions are often aided greatly by the calculation abilities of computers and can involve thousands of calculations resulting in a long list of numbers which then can be formulated into an **approximation** (Neumann 2004). Experimental solutions are as the name implies, solutions which are acquired through experimental data and or observation (empirical solution).

1.2 Benefits and Limitations of the Closed Form Solution

Depending on subject, numerical solutions can give more accurate results than their closed form counterparts, particularly because the mathematics involved would become too tedious and/or complex to perform analytically. That is not to say that with today's modern computers and programs that analytical solutions in these situations are obsolete, as they still very much provide a wide range of uses and values of which numerical solutions do not possess.

A way in which one may understand these benefits is to look deeper into the structure of the closed form solution. The closed-form solution involves an understanding of the definitions of the system parameters and the product/s of their interactions, and the combination of this information to reach a desired conclusion. This is an integral process in solving physical processes analytically and an effective way in understanding their true nature as it can unveil the limitations and assumptions made. It is through this fundamental structure that it may be said closed form solutions offer an advantage over numerical solutions, as the analysis of a system and the interactions of its components is one which can yield great insight. One can examine an equation, alter it, incorporate it; as methods to see the interconnections and intricacies of the processes within it.

Closed form solutions also possess other advantages. Given that many closed form solutions are purely mathematical in form, it is then permissible to subject it to the many operations and manipulations which encompass mathematics. This flexibility allows the possibilities for closed-form solutions to morph into solutions for related problems. Furthermore, due to its synthesis from the raw components of a system it can also be used for validation, though one should be mindful of the simplifying assumptions involved in these solutions. Such assumptions are a major limitation of the closed form solution, however they are a necessary accommodation as without

them, solving more complicated models analytically may become impracticable or even impossible. In situations where higher accuracy is required or the model has become too complex to allow for the application of analytical solutions, numerical solutions are of preference.

The exploration of such qualities and the overall values of the closed-form solution in geotechnical problems is a **major objective** of this dissertation. In addition to this, the **secondary objective** is to explore the relationships between selected geotechnical solutions and their capabilities, which will be introduced over the coming chapters.

Chapter 2

Introduction to 2D Models

This thesis will center around the 2D analysis of geotechnical problems, relevant to one area in particular the plane theory of elasticity. The elastic property of a material relates to its deformational response under loading. If the material returns to its original state once the forces are removed it is known as *perfectly elastic* (Timoshenko & Goodier 1951). Whether or not a solid does this is ultimately due to its atomic properties but this aspect will not be considered in this thesis.

Soil is not an elastic material however treating it as such allows the use of solutions and methods of analysis for calculating stresses and strains in response to applied forces (Powrie 2004, pp.329). By selecting the right elastic parameters, elastic analysis on soil masses can still provide reasonable results (Powrie 2001, pp.321). Two dimensional elasticity consists of two general types of planar analysis, plane strain and plane stress.

Elastic parameters related to this type of analysis are.

Young's Modulus

$$E = \sigma/\epsilon$$

Shear Modulus

$$G = \tau_{xy}/\gamma_{xy}$$

Poisson's Ratio

$$\nu = \epsilon_{transverse}/\epsilon_{axial}$$

In modern times finite element packages are a very effective means for solving linear elastic boundary value problems (Bower 2008). However exact solutions are of practical importance in areas such as; contact problems, stress concentrations, thermal stress problems, solutions for cracks and dislocations in solids (Bower 2008).

2.1 Plane Strain

For this thesis the general symbolical and terminological constructs will be adopted for both stress and strain. An elongation is denoted by the Greek letter ϵ (epsilon) and a shearing strain is represented by γ (gamma) with subscripts denoting the direction, see Figure 2.1.

Plane strain is a common simplification in geomechanics because often the there is one dimension that is very large when compared to the other dimensions (Timoshenko & Goodier 1951). This could be a wall, embankment or excavation which

is extremely long in comparison to its height and width, the assumption is that the strain in the longitudinal direction is zero (Powrie 2004, pp.70). The principle of plane strain may only be applied when there are no significant changes in cross sectional dimensions or loadings.

For example taking the cross section of an extremely long embankment and the z axis as the longitudinal direction; the z dimension is so large when compared to the other dimensions any strain (a ratio of its deformed length over its original length) will be so small that it can be deemed negligible and therefore ϵ_z, γ_{xz} and γ_{yz} would be approximately equal to 0. The application of plane strain greatly simplifies any subsequent stress analysis on the body (Powrie 2004, pp.70). See Figure 2.1 for a diagrammatic representation of plane strain.

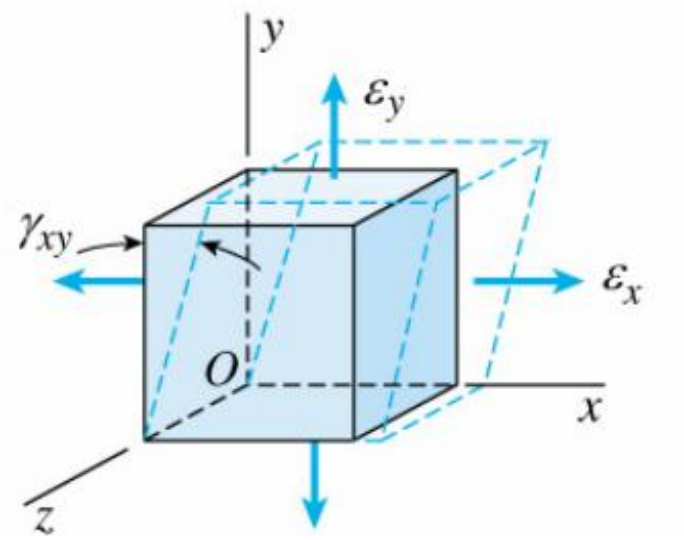

Figure 2.1: Plane Strain (Source: http://academic.uprm.edu/pcaceres/Courses/MechMet/MET-2B.pdf

2.2 Plane Stress

A stress that is normal to the plane is denoted by the Greek letter σ (sigma). A stress which acts parallel to the plane is denoted by the Greek letter τ(tau). Axial subscripts are used to denote the planar direction in which these stresses act, for example a subscript of σ_x means a normal stress, acting parallel to the x-axis (Timoshenko & Goodier 1951). For τ_{xy} the first letter indicates that the stress is normal to the x axis and the second letter indicates that it is in the same direction as the y axis.

Plane stress similarly to plane strain suggests the negligence or nullification of normal and shear stress in one axial direction. Typically a state of plane stress occurs when one dimension is very small relative to the others. A related example could be the stresses on a thin plate submerged in soil media.

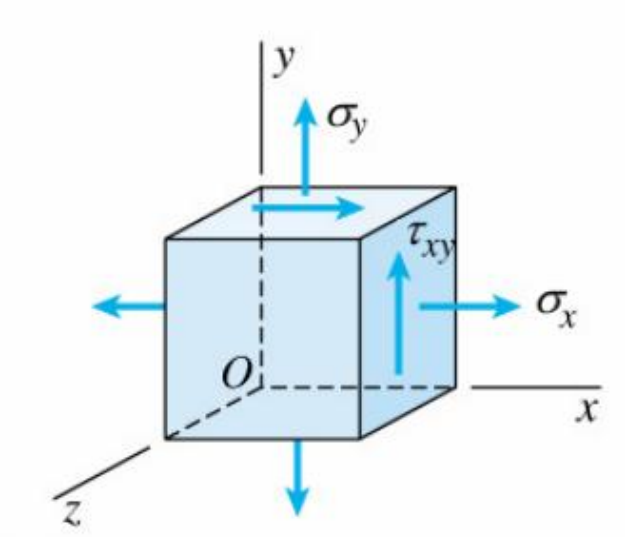

Figure 2.2: Plane Stress (Source: http://academic.uprm.edu/pcaceres/Courses/MechMet/MET-2B.pdf)

In soil mechanics compressive stresses and strains are usually taken as positive and shear stresses and associated strains which create a clockwise moment about an

exterior point to the plane being considered will be taken as positive (Perloff & Baron 1976, pp.55). These conventions will be adopted in this thesis.

2.3 Axisymmetric Models

Powrie (2004, pp.71) states that when stress and strain conditions on a plane have rotational symmetry about the vertical axis it can be termed **axisymmetric**. Like plain strain, when a body satisfies axisymmetry stress analysis is greatly simplified. On occasions where a problem is restricted from featuring either of these simplifications numerical solutions are usually required such as finite element or finite difference analysis (Powrie 2004, pp.71).

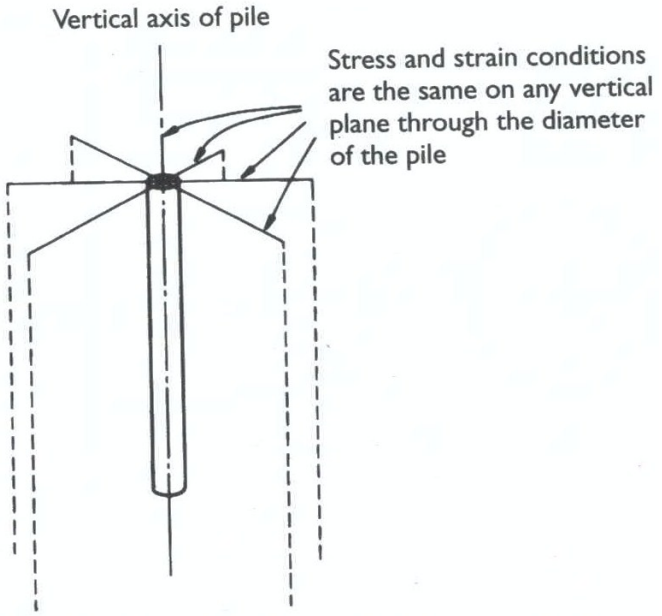

Figure 2.3: Stress strain axisymmetry of a pile (Powrie 2004, pp.71).

In geomechanics this principle can typically be applied to circular subsurface objects. Axisymmetry is a convenience as it can provide a simplification of the relationships between variables. For example taking an axisymmetric loading around the circumference of a circular tunnel simplifies the relationship between tunnel

loading and spatial dimensions. Using the same example axisymmetric soil conditions surrounding the tunnel would eliminate the significance of the location of the cross section taken.

Chapter 3

Solutions for Stress in Soil Masses and their Applications

3.1 Introduction

This chapter sets the foundation for the area of Geotechnical Engineering in which this paper focuses, *stress in soil masses*. Three solutions for linear elasticity problems have been selected. The three solutions that have been selected are all closely related yet are individualised in terms of their load placements. The first of the solutions was developed by Lord Kelvin (1824-1907) a physicist and engineer, for a point load acting within an infinite elastic mass. The second by Joseph Boussinesq (1842-1929) a French physicist, for a point load acting on the surface of a linear elastic semi-infinite mass. The third by Raymond D. Mindlin (1906-1987) for a point load acting beneath the surface of a semi-infinite mass.

All three solutions assume a homogeneous, isotropic, elastic medium. A material is said to be **homogeneous** when its physical properties are identical at all points within its boundaries and it is said to be **isotropic** when the elastic properties

of the material are the same in all directions (Timoshenko & Goodier 1951). In reality absolute homogeneity and isotropy are both unlikely but the assumptions can still provide accurate results as long as the geometric dimensions of the body under study are large enough so that internal inconsistencies may be averaged out (Timoshenko & Goodier 1951). In Geomechanics any vast discrepancies in soil properties would need to be taken into account.

3.2 Kelvin's Solution

In 1848 Lord Kelvin devised a solution for the stresses produced from a load acting within the interior of an infinite mass.

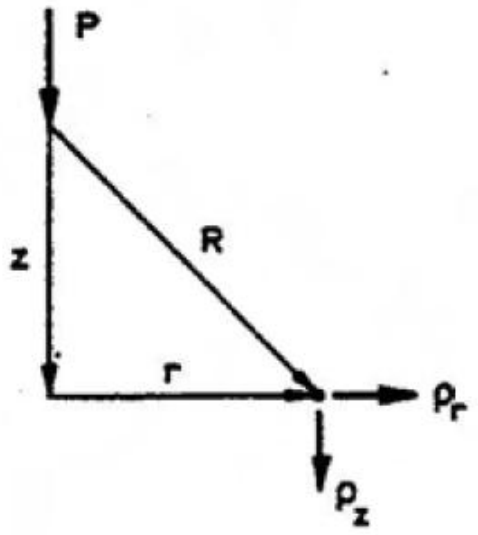

Figure 3.1: Kelvin's Solution for a point load P in an infinite elastic space (Poulos & Davis 1974, pp.16).

His solution for normal stresses consisted of the following (Poulos & Davis 1974,

pp.16).

$$\sigma_z = \frac{P}{8\pi(1-\nu)}\left[\frac{3z^3}{R^5} + \frac{(1-2\nu)z}{R^3}\right] \tag{3.1}$$

$$\sigma_r = \frac{P}{8\pi(1-\nu)}\frac{z}{R^3}\left[\frac{-3r^2}{R^2} - (1-\nu)\right] \tag{3.2}$$

$$\sigma_\theta = -\frac{P(1-2\nu)}{8\pi(1-\nu)}\frac{z}{R^3} \tag{3.3}$$

and for displacement,

$$\rho_z = \frac{P(1+\nu)}{8\pi(1-\nu)ER}\left[3 - 4\nu\frac{z^2}{R^2}\right] \tag{3.4}$$

$$\rho_r = -\frac{P(1+\nu)}{8\pi(1-\nu)E} \cdot \frac{rz}{R^3} \tag{3.5}$$

where subscripts r,z and θ indicate direction. θ is the circumferential direction, perpendicular to both r and z

As Kelvin's problem excludes a surface, the practical applications of this particular solution are limited. Kelvin's solution can be integrated to determine distributed loads.

3.3 Boussinesq's Solution

In 1885 Boussinesq solved the problem involving a point load acting at the surface of an elastic **half space** (a body of infinite depth and width, also known as a semi-infinite domain) to find the stress and strains at any point within it (Powrie 2004, pp.336).

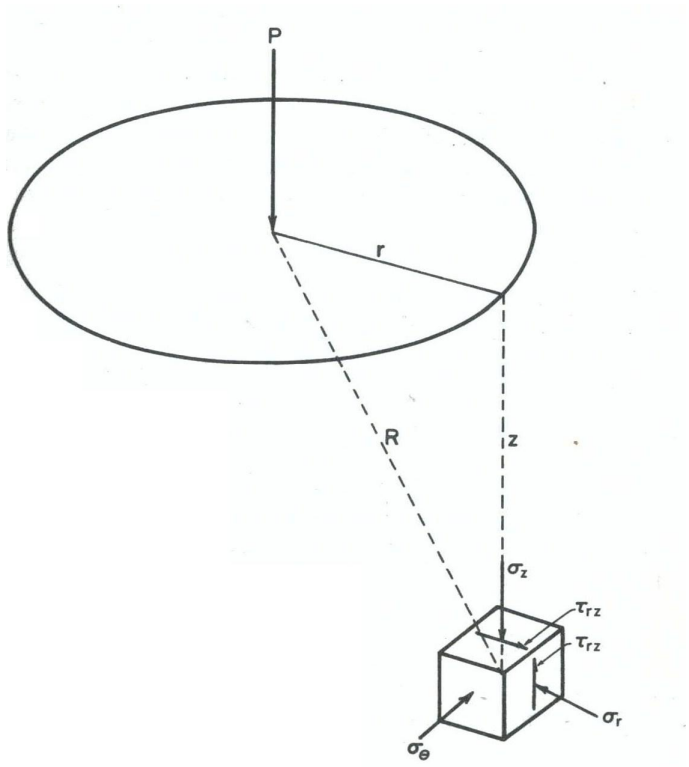

Figure 3.2: Boussinesq's solution for a point load P acting at the surface of a semi-infinite elastic space (Perloff & Baron 1976, pp.179).

Referring to the figure above, the Boussinesq solution consists of the following equations for normal stress (Poulos & Davis 1974, pp.16).

$$\sigma_z = \frac{3Pz^3}{2\pi R^5} \tag{3.6}$$

$$\sigma_r = -\frac{P}{2\pi R^2}\left[\frac{-3r^2 z}{R^3} - \frac{(1-2\nu)R}{R+z}\right] \tag{3.7}$$

$$\sigma_\theta = -\frac{(1-2\nu)R}{2\pi R^2}\left[\frac{z}{R} - \frac{R}{R+z}\right] \tag{3.8}$$

and for displacement,

$$\rho_z = \frac{P(1+\nu)}{2\pi E R}\left[2(1-\nu) + \frac{z^2}{R^2}\right] \tag{3.9}$$

$$\rho_r = \frac{P(1+\nu)}{2\pi E R}\left[\frac{rz}{R^2} - \frac{r(1-2\nu)}{R+z}\right] \tag{3.10}$$

where subscripts r,z and θ indicate direction. θ is the circumferential direction, perpendicular to both r and z. Due to the fact that many geotechnical engineering tasks take place on the surface these equations are extremely useful. Like Kelvin's solution, Boussinesq's equations can also be integrated to facilitate for line loads and area loads.

3.4 Mindlin's Solution

In 1936 Raymond D. Mindlin developed a solution of the three dimensional elasticity equations for a homogeneous, isotropic, semi-infinite solid with a force acting in its interior (Mindlin 1936).

Kelvin and Boussinesq had both reached fundamental results in this area prior to Mindlin's development. Both of their solutions had a range of practical uses, but Mindlin still saw room for advancement. Mindlin described his paper as a solution

that would fill in the gap between these two solutions, giving the stresses for a case where the force is applied *near*, not above nor irrespective of a surface (Mindlin 1936).

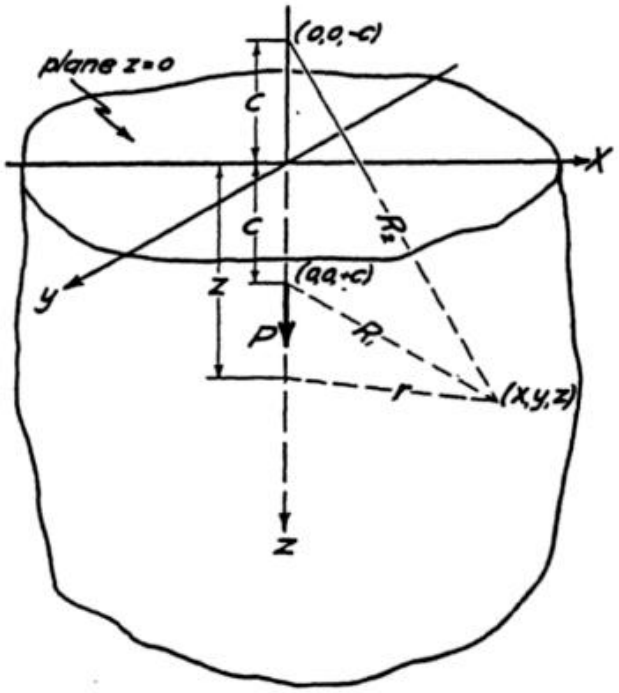

Figure 3.3: Mindlin's solution for a force normal to the boundary in the interior of a semi-infinite mass (Mindlin 1936).

This highlights an important differentiation between Mindlin's solution and Kelvin's solution, that Mindlin introduces a plane boundary which opens it up to a range of practical applications whilst still retaining the possibility of reaching the same results as Kelvin's solution (Mindlin 1936).

In his original paper Mindlin divided his solution into two parts, one solution for a vertical point load perpendicular to the surface and another for a horizontal point load parallel with the surface.

Mindlin's solution for the normal stresses created by a point load perpendicular to

the surface involves the following equations (Poulos & Davis 1974, pp.16).

$$\begin{aligned}\sigma_x = &- \frac{P}{8\pi(1-\nu)}\left[\frac{(1-2\nu)(z-c)}{R_1^3} - \frac{3x^2(z-c)}{R_1^5} + \frac{(1-2\nu)[3(z-c)-4\nu(z+c)]}{R_2^3}\right.\\ &- \frac{3(3-4\nu)x^2(z-c)-6c(z+c)[(1-2\nu)z-2\nu c]}{R_2^5} - \frac{30cx^2z(z+c)}{R_2^7}\\ &\left.- \left(\frac{4(1-\nu)(1-2\nu)}{R_2(R_2+z+c)}\right)\left(1-\frac{x^2}{R_2(R_2+z+c)}-\frac{x^2}{R_2^2}\right)\right]\end{aligned} \tag{3.11}$$

$$\begin{aligned}\sigma_y = &- \frac{P}{8\pi(1-\nu)}\left[\frac{(1-2\nu)(z-c)}{R_1^3} - \frac{3y^2(z-c)}{R_1^5} + \frac{(1-2\nu)[3(z-c)-4\nu(z+c)]}{R_2^3}\right.\\ &- \frac{3(3-4\nu)y^2(z-c)-6c(z+c)[(1-2\nu)z-2\nu c]}{R_2^5} - \frac{30cy^2z(z+c)}{R_2^7}\\ &\left.- \left(\frac{4(1-\nu)(1-2\nu)}{R_2(R_2+z+c)}\right)\left(1-\frac{y^2}{R_2(R_2+z+c)}-\frac{y^2}{R_2^2}\right)\right]\end{aligned} \tag{3.12}$$

$$\begin{aligned}\sigma_z = &- \frac{P}{8\pi(1-\nu)}\left[-\frac{(1-2\nu)(z-c)}{R_1^3} + \frac{(1-2\nu)(z-c)}{R_2^3} - \frac{3(z-c)^3}{R_1^5}\right.\\ &\left.- \frac{3(3-4\nu)z(z+c)^2-3c(z+c)(5z-c)}{R_2^5} - \frac{30cz(z+c)^3}{R_2^7}\right]\end{aligned} \tag{3.13}$$

Furthermore noting axisymmetry for the case of vertical load, instead of two formulae σ_x and σ_y, it can be exemplified by one formula σ_r.

$$\begin{aligned}\sigma_r = &- \frac{P}{8\pi(1-\nu)}\left[\frac{(1-2\nu)(z-c)}{R_1^3} - \frac{(1-2\nu)(z+7c)}{R_2^3} + \frac{4(1-\nu)(1-2\nu)}{R_2(R_2+z+c)}\right.\\ &- \frac{3r^2(z-c)}{R_1^5} + \frac{6c(1-2\nu)(z+c)^2-6c^2(z+c)-3(3-4\nu)r^2(z-c)}{R_2^5}\\ &\left.- \frac{30cr^2z(z+c)}{R_2^7}\right]\end{aligned} \tag{3.14}$$

and for displacement,

$$\begin{aligned}\rho_z =& \frac{P}{16\pi G(1-\nu)}\left[\frac{3-4\nu}{R_1}+\frac{8(1-\nu)^2-(3-4\nu)}{R_2}+\frac{(z-c)^2}{R_1^3}\right.\\ &\left.+\frac{(3-4\nu)(z+c)^2-2cz}{R_2^3}+\frac{6cz(z+c)^2}{R_2^5}\right]\end{aligned} \tag{3.15}$$

$$\begin{aligned}\rho_r =& \frac{Pr}{16\pi G(1-\nu)}\left[\frac{z-c}{R_1^3}+\frac{(3-4\nu)(z-c)}{R_2^3}-\frac{4(1-\nu)(1-2\nu)}{R_2(R_2+z+c)}\right.\\ &\left.+\frac{6cz(z+c)}{R_2^5}\right.\end{aligned} \tag{3.16}$$

Where,

$$r = \sqrt{x^2+y^2}$$

$$R_1 = \sqrt{r^2+(z-c)^2}$$

$$R_2 = \sqrt{r^2+(z+c)^2}$$

3.5 Applications in Geotechnical Problems

This section provides a review of literature on the applications of closed form Mindlin's, Boussinesq's and Kelvin's solutions. There has been many numerical methods developed referencing these solutions but as this thesis centres on analytical solutions these papers will not be reviewed. Additionally papers which involve anisotropic or non-homogeneous media will not be considered as the solutions discussed in this thesis are specifically formulated for an isotropic, homogeneous medium.

3.5.1 Applications in Piling

As piles are generally inserted into the ground for the support and stability of structures they are responsible for the transmission of heavy loadings into the soil beneath. Pile analysis is a major civil engineering problem and one in which elasticity theory has been used as a method to analyse piles and pile groups.

In their 1971 paper Butterfield and Banerjee performed an elastic analysis of rigid and compressible piles and pile groups based on the use of Mindlin's solution in a homogeneous isotropic medium. Through integration of Mindlin's point load solutions they were able to obtain insight into the relationships between certain variables within the system.

The study observed the effect of variations in the ratio of pile length to pile diameter, the ratio of modulus of elasticity of the pile to shear modulus of the medium of which it is situated and the effect that enlarging the base has on the load displacement characteristics of singular piles. When Butterfield and Banerjee compared their results with published approximate solutions and laboratory tests they found them to be close enough to warrant the use of their solution for the calculation of pile group settlement ratios and the prediction of pile group behaviour based on single pile load displacement data.

Comparisons between Mindlin's solution and Boussinesq's solution for the stresses resulting from distributed subsurface loadings (triangular and rectangular) were studied by Geddes in 1966. While Mindlin's solution was applied successfully it was found that if Boussinesq's solution was adopted significant overestimates were produced (Geddes 1969). This is because Boussinesq's solution is not designed for subsurface loading.

Geddes (1969) modified the Boussinesq solution to include subsurface loading catering for vertical skin friction forces in piles. A limitation being that it does not

take into account the presence of overburden loading as the solution is based on the Boussinesq solution which acts at the surface. Therefore in general Geddes' solution will produce overestimates for stress. As the solution was intended for approximation purposes this inaccuracy is only a minor limitation.

Tian-quan (1981) detailed pile analysis on both rigid and compressible piles by using two simple integral equation methods. The first consisting of a horizontal Mindlin force distributed along an axis combined with a Boussinesq point force and the second consisting of a a distributed vertical Mindlin force (Tian-quan 1981). The paper was able to transform a three dimensional problem into a one dimensional Fredholm integral equation of the first kind.

3.5.2 Applications in Anchoring

Similarly to piling, Earth or ground anchors are a foundation providing support and stability for certain structures. Anchors are tensile members as there are usually tensile forces involved, anchoring in place whilst undergoing uplift forces or horizontal pull out forces (Altun, Karakan and Caglar Tuna 2013). Sub-surface loadings such as these open up anchoring problems to analysis via Mindlin's solution. Furthermore some anchors provide an opposite force acting at the surface compressing the soil, such as a plate, in this case Boussinesq's solution may be used. Having both tensile and compressive forces working together can improve the support offered by the anchor so for some designs it may be preferable to have both, thus it may be possible to analyse an anchor system involving a combination of both Mindlin's and Boussinesq's solutions.

Many of the following applications are more related to contact mechanics which strays somewhat further away from the more traditional civil and geotechnical engineering applications discussed in other sections. Nonetheless they represent an important and well researched area on the application of the selected elasticity

solutions whilst often containing problems in relation to ground anchors.

Selvadurai (1979) formulated a closed form solution based on Mindlin's equations for the displacement experienced by a rigid circular plate connected to a ground anchor. The problem involved an isotropic, elastic half-space subject to axisymmetric internal and external loads (see Figure 3.4) (Selvadurai 1979). The analysis contained a variety of distributed loading cases, constant, linear and parabolic; neglecting any effects of friction (Selvadurai 1979). The paper also suggests that this particular problem has useful connections with rock anchoring and in situ testing.

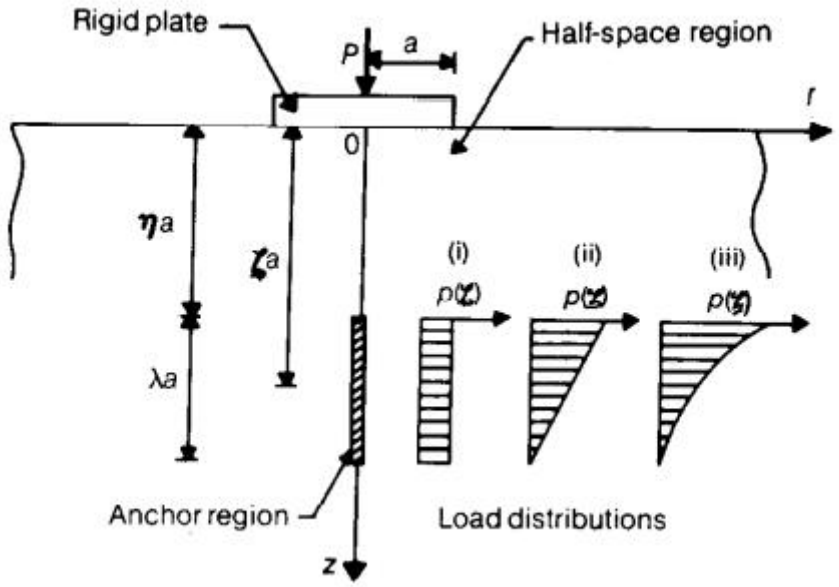

Figure 3.4: Selvadurai's anchored rigid circular plate (Selvadurai 1979).

In their 2013 research paper, Altun, Karakan and Caglar Tuna followed on from Salvarudai's 1979 work, analysing the *load-displacement* relationship for a rigid ground anchored circular plate using Mindlin's solution. The effects of anchor length, anchor depth and the type of load distribution has on the load-displacement relationship was also observed (Altun et al. 2013).

For verification purposes Altun, Karkan and Caglar Tuna also undertook FEM

(Finite Element Method) analysis and compared it with their analytical results. It was found that the two methods did not agree well for Mindlin's problem and that the reasoning for this was due to discrepancies in the solution procedures and the material properties assigned in each method (Altun et al. 2013). In spite of these disagreements it is suggested that the analytical solutions to determine anchor displacements may still be applicable as long as it is in the case of an ideal soil and the elastic parameters are determined correctly (Altun et al. 2013).

3.5.3 Applications in Tunnelling

Tunnels are often a part of engineering projects in areas such as transport, public health and mining engineering. Tunnels have been subjected to research in which elastic analysis including Mindlin's solution has been performed in order to predict nearby soil displacements and to examine the effect of stresses on places of interest in the proximity. Such analysis could theoretically be performed on other underground excavations such as caverns or shafts.

Zhang et al. (2013) utilised a semi-analytical approach for geotechnical tunnel analysis where the tunnel was assumed as an elastic beam. An integrated Boussinesq's solution was used to determine the distributed soil stresses and tunnel displacement induced by an adjacent excavation. Additionally, through integration of Mindlin's solution, Zhang et al. (2013) was able to estimate the resistance of a tunnel. Their work is founded on the contemporary challenges of incorporating metro systems into urban areas, as the interaction between underground structures and existing tunnels represents a significant safety concern.

Among the results were the effects of different factors on heave displacement (*heaving* of a tunnel happens due to the rebound of soil when adjacent soil is excavated), these included excavation area, relative distance and construction procedure (Zhang et al. 2013). A good conformity was found when the displacement

results were verified against the field measurements for deep excavations above metro tunnels (Zhang et al. 2013).

Among the limitations of the semi-analytical method, Zhang et al. (2013) noted that it was best used for quick assessment of tunnel displacement and for higher accuracy numerical analysis should be utilised. Additionally clarification is needed as to whether or not this method may be applied when soil properties change with time, take for example soft clays (Zhang et al. 2013).

Chow (1994, p.16) used Mindlin's solution for finding the surface displacement in a shallow tunneling problem (see figure 3.5). Chow postulated that the total vertical displacement at point O could be found through integrating equation 3.15 along the y axis from $-\infty$ to $+\infty$.

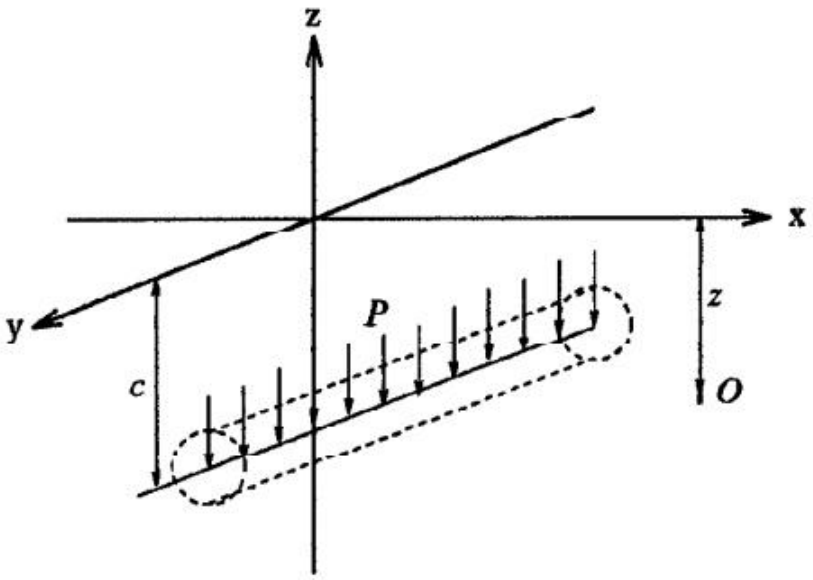

Figure 3.5: Tunnel problem (Chow 1994, pp.16).

In the paper a solution was reached which could not be evaluated analytically (and hence exact surface displacements could not be found). After reformulating the approach, *relative surface displacements* were found by comparing displacements at two points (Chow 1994).

3.5.4 Applications in Contact Mechanics

Mindlin's solution has been used in a wide range of research in contact problems. Selvadurai (2001) analysed via Mindlin's problem for a half space bonded with a thin plate of infinite extent at the surface subject to an axisymmetric load. The aim of such an analysis is to identify and develop integral expressions for the influence a Mindlin force has on deflections and moments inside the plate (Selvadurai 2001).

Rahman and Newaz (2000) modelled a Boussinesq type solution for a load acting at the surface of an isotropic half-space in which the surface had been coated with a thin soft film. The applications for this research are more tuned to mechanical areas with such examples given as magnetic layer protection for hard disk files and thermal protection in aerospace design (Rahman & Newaz 2000). In general, the results may be useful in determining solutions for frictionless contact problems where the surface is reinforced by thin coatings (Rahman & Newaz 2000).

3.5.5 General Research and Applications

Sun et al. (2013) developed an extended, integrated form of Mindlin's displacement equations to find displacements at an arbitrary point induced by horizontally or vertically distributed loading acting normally or tangentially. The results were compared and found to correlate well with existing literature in the area (Sun et al. 2013).

Sun et al. (2013) indicate that the formulae can be used to understand displacement fields around embedded structures in practical situations and furthermore may be useful in the development of future computer programs in the area.

Basile (2002) presented the integration for a singular Mindlin displacement solution over a cylindrical surface. The derivation of the equation is presented in

full. Such analytical solutions are helpful in reducing computational resources required in certain analyses (Basile 2002). Likewise Douglas and Davis (1964) integrated Mindlin's horizontal displacement equations in order to attain values for the displacement and rotation of a vertically buried footing subject to moment and horizontal loadings. Ultimately this solution was used in a numerical method, however this paper is still somewhat relevant to this thesis as the integration of Mindlin's solution is displayed.

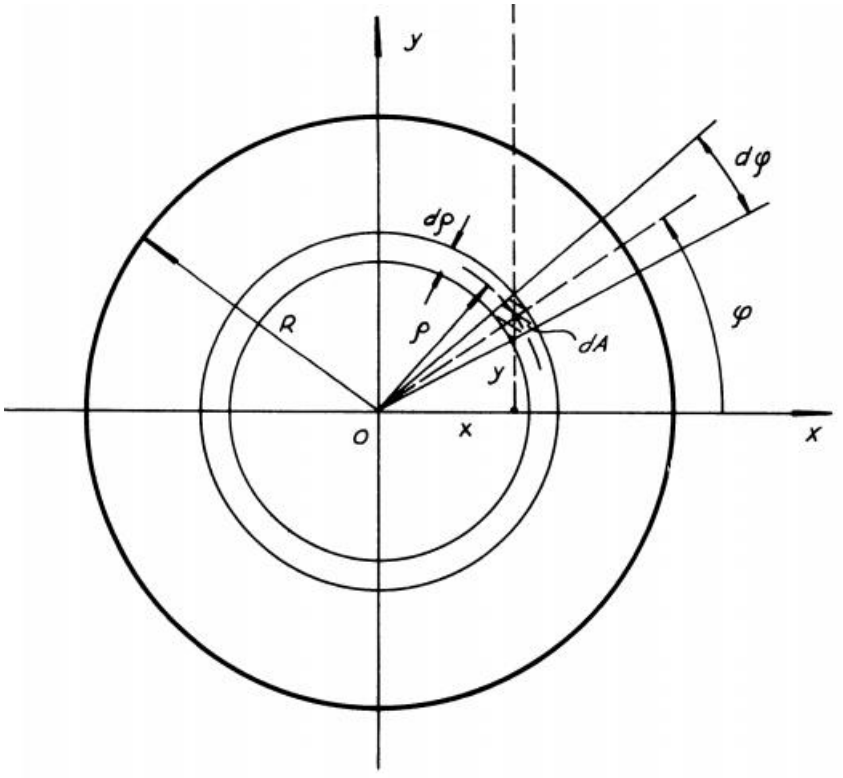

Figure 3.6: Dominguez (1966) detailed how the stress due to a uniform distributed load over the area of the shaded section above could be found through integration.

Dominguez (1966) showed the steps involved in integrating Boussineq's equation for normal stress along the x,y,z axes for both horizontal and vertical loadings over a radial area (see Figure 3.6). Dominguez's expressions are also fairly flexible as can be seen from Figure 3.6 in that it allows the disregard of certain segments of the circle based on input radius (ρ) and the angular span (ϕ).

The expressions developed by Dominguez could be further built upon or used in subsequent analysis. Dominguez's integrated Boussinesq's solution is used as a calculation check in Chapter 4.

Acknowledging the previously published results by Poulos Davis (1974), Vaziri et al. (1982) produced the integrated forms of Mindlin's displacement equations in both the x and z directions for both horizontal and vertical loadings. Through integrating these equations Vaziri et al. produced the expressions for the displacements due to a uniform shear stress as well as displacements produced by a uniformly distributed pressure. The motivation behind this research was to assist in the development of a computer program for retaining walls (Vaziri et al. 1982). Vaziri et al. (1982) validated the integrated solutions using a variety of techniques which found them to be correct.

3.5.6 Summary of Applications

Overall there is by no means a large amount of literature on this topic area. The literature reviewed in this section makes heavy use of both Boussinesq's and Mindlin's solutions over a variety of applications mainly piling, anchoring and tunnelling. As these were the main areas of application, they will serve as first preference when exploring possible new analytical calculations within them.

It is also worth noting the absence of Kelvin's solution in the literature. The reason for this is most likely due to the limited practical value of Kelvin's solution. Nonetheless it is still an important solution as it set the foundation for both Boussinesq and Mindlin to build upon in the formulation of their own solutions.

Chapter 4

Circular Sub-Surface Loading

4.1 Introduction

Now that the abilities and possible areas of application of the chosen solutions have been identified this chapter serves as an exploration into some of the possible applications which have not yet been covered in literature. The calculations presented here can further undergo subsequent analysis against their numerical counterparts in order to determine their true value, both in general and due to its analytical form.

4.2 Integration of Mindlin's Solution for a Uniformly Distributed Sub-Surface Circular Load

While much of the covered literature (Geddes 1966, Vaziri et al. 1982, Basile 2002, Zhang et al. 2013, Douglas Davis 1964) included developed integrated Mindlin's solutions for sub-surface loadings; these publications do not all explicitly show

the integration process nor state the fully integrated solution. Additionally there appears to be an emphasis on integrating Mindlin's displacement equations whilst the integration of Mindlin's original stress equations appear to have not yet been published. Geddes (1966) did include and show the integration of Mindlin's stress equations however it was a modified version to cater for numerical applications.

This section contains the integration of the original normal stress equation developed by Mindlin as well as a possible ways in which it can be applied.

Figure 4.1 illustrates a potential area of exploration for the integrated form of Mindlin's equation for normal stress generated by a vertical force.

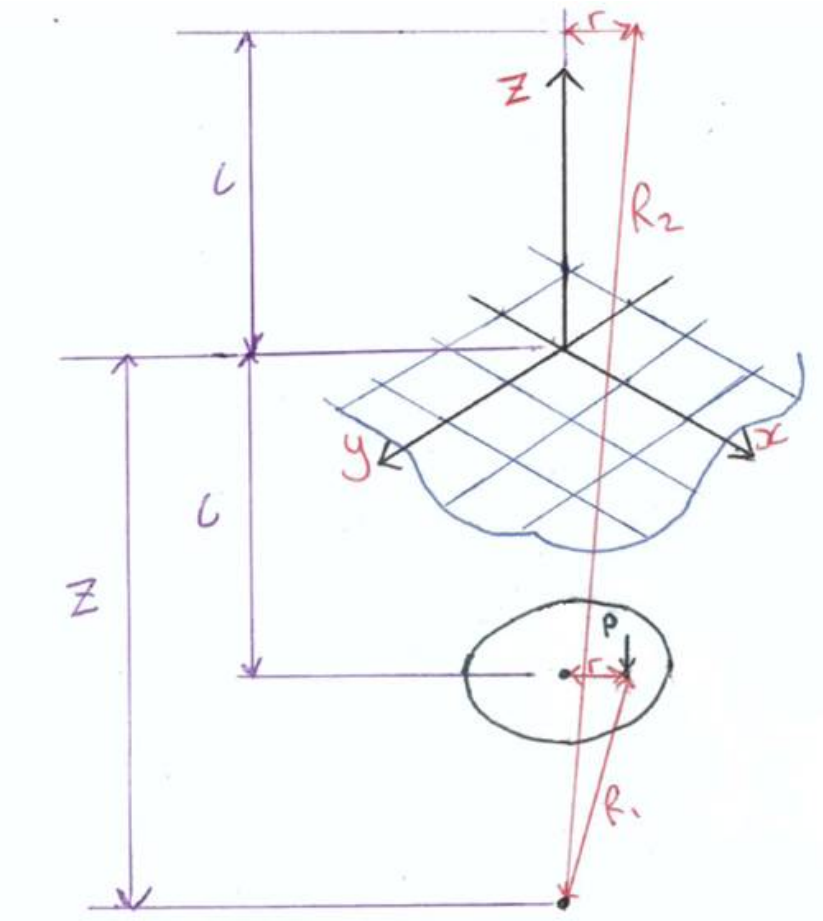

Figure 4.1: A uniformly distributed vertical circular loading beneath the surface (x-y plane).

Taking Mindlin's equation for normal stress in the z direction,

$$\sigma_z = -\frac{P}{8\pi(1-\nu)}\left[-\frac{(1-2\nu)(z-c)}{R_1^3}+\frac{(1-2\nu)(z-c)}{R_2^3}-\frac{3(z-c)^3}{R_1^5} - \frac{3(3-4\nu)z(z+c)^2-3c(z+c)(5z-c)}{R_2^5}-\frac{30cz(z+c)^3}{R_2^7}\right] \tag{4.1}$$

and integrating with respect to r and integrating again with respect to θ (angle in radians), we can find σ_z induced by a uniformly loaded circular area, with a load per unit area of q and a radius of R,

$$\sigma_z = \int_0^{2\pi}\int_0^R -\frac{q\cdot r\cdot dr\cdot d\theta}{8\pi(1-\nu)}\left[-\frac{(1-2\nu)(z-c)}{R_1^3}+\frac{(1-2\nu)(z-c)}{R_2^3}-\frac{3(z-c)^3}{R_1^5} - \frac{3(3-4\nu)z(z+c)^2-3c(z+c)(5z-c)}{R_2^5}-\frac{30cz(z+c)^3}{R_2^7}\right] \tag{4.2}$$

$$\sigma_z = -\frac{q}{8\pi(1-\nu)}\int_0^{2\pi} d\theta\int_0^R r\cdot dr\left[-\frac{(1-2\nu)(z-c)}{R_1^3}+\frac{(1-2\nu)(z-c)}{R_2^3}-\frac{3(z-c)^3}{R_1^5} - \frac{3(3-4\nu)z(z+c)^2-3c(z+c)(5z-c)}{R_2^5}-\frac{30cz(z+c)^3}{R_2^7}\right] \tag{4.3}$$

Remembering,

$$R_1 = \sqrt{r^2+(z-c)^2}$$

$$R_2 = \sqrt{r^2+(z+c)^2}$$

These integrations can be based upon the already solved integrals by Dwight (1957). In Dwight (1957) the solutions to the following integrals are outlined, all of which are relevant to Eq. 4.3.

$$\int \frac{a \cdot da}{\sqrt{a^2 + b^2}^3} = \frac{-1}{\sqrt{a^2 + b^2}} \tag{4.4}$$

$$\int \frac{a \cdot da}{\sqrt{a^2 + b^2}^5} = \frac{-1}{3\sqrt{a^2 + b^2}^3} \tag{4.5}$$

$$\int \frac{a \cdot da}{\sqrt{a^2 + b^2}^7} = \frac{-1}{5\sqrt{a^2 + b^2}^5} \tag{4.6}$$

For this calculation we are considering a full circular load, therefore $\theta = 2\pi$, so instead of detailing the second integration, the final solution will simply be multiplied by 2π to achieve the same effect. We then divide Eq. 4.2 up into separate terms to ease integration and substituting equations for R_1 and R_2.

For the first term, as this is effectively the integral in Eq. 4.4 it can be solved following that process which gives,

$$[-(1-2\nu)(z-c)] \int_0^R \frac{r \cdot dr}{\sqrt{r^2 + (z-c)^2}^3} = [-(1-2\nu)(z-c)] \left[\frac{-1}{\sqrt{r^2 + (z-c)^2}} \right]_0^R \tag{4.7}$$

Following the same process the 2nd term becomes,

$$[(1-2\nu)(z-c)] \int_0^R \frac{r \cdot dr}{\sqrt{r^2 + (z+c)^2}^3} = [(1-2\nu)(z-c)] \left[\frac{-1}{\sqrt{r^2 + (z+c)^2}} \right]_0^R \tag{4.8}$$

Integrating the 3rd term with assistance from equation 4.5, results in

$$[-3(z-c)^3]\int_0^R \frac{r\cdot dr}{\sqrt{r^2+(z-c)^2}^5} = -3(z-c)^3\left[\frac{-1}{3\sqrt{r^2+(z-c)^2}^3}\right]_0^R \tag{4.9}$$

Integrating the 4th term with assistance from equation 4.5, results in

$$-m\int_0^R \frac{r\cdot dr}{\sqrt{r^2+(z+c)^2}^5} = -m\left[\frac{-1}{3\sqrt{r^2+(z+c)^2}^3}\right]_0^R \tag{4.10}$$

where

$$m = 3(3-4\nu)z(z+c)^2 - 3c(z+c)(5z-c)$$

Integrating the 5th term with assistance from equation 4.6, results in

$$-30cz(z+c)^3\int_0^R \frac{r\cdot dr}{\sqrt{r^2+(z+c)^2}^7} = -30cz(z+c)^3\left[\frac{-1}{5\sqrt{r^2+(z+c)^2}^5}\right]_0^R \tag{4.11}$$

Combining all of these results and simplifying the following is achieved,

$$\begin{aligned}\sigma_z = -\frac{q}{4-4\nu}\Bigg[&\left[\frac{(1-2\nu)(z-c)}{\sqrt{r^2+(z-c)^2}}\right]_0^R - \left[\frac{(1-2\nu)(z-c)}{\sqrt{r^2+(z+c)^2}}\right]_0^R + \left[\frac{(z-c)^3}{\sqrt{r^2+(z-c)^2}^3}\right]_0^R \\ &+ \left[\frac{m}{3\sqrt{r^2+(z+c)^2}^3}\right]_0^R + \left[\frac{6cz(z+c)^3}{\sqrt{r^2+(z+c)^2}^5}\right]_0^R\Bigg]\end{aligned}$$

Finally we obtain

$$\begin{aligned}\sigma_z = -\frac{q}{4-4\nu}\Bigg[&\left[\frac{(1-2\nu)(z-c)}{\sqrt{R^2+(z-c)^2}}\right] - \left[\frac{(1-2\nu)(z-c)}{\sqrt{(z-c)^2}}\right] - \left[\frac{(1-2\nu)(z-c)}{\sqrt{R^2+(z+c)^2}}\right] \\ &+ \left[\frac{(1-2\nu)(z-c)}{\sqrt{(z+c)^2}}\right] + \left[\frac{(z-c)^3}{\sqrt{R^2+(z-c)^2{}^3}}\right] - \left[\frac{(z-c)^3}{\sqrt{(z-c)^2{}^3}}\right] \\ &+ \left[\frac{m}{3\sqrt{R^2+(z+c)^2{}^3}}\right] - \left[\frac{m}{3\sqrt{(z+c)^2{}^3}}\right] + \left[\frac{6cz(z+c)^3}{\sqrt{R^2+(z+c)^2{}^5}}\right] - \left[\frac{6cz(z+c)^3}{\sqrt{(z+c)^2{}^5}}\right]\Bigg]\end{aligned} \tag{4.12}$$

where

$$m = 3(3-4\nu)z(z+c)^2 - 3c(z+c)(5z-c)$$

4.2.1 Comparing Integrated Mindlin's and Boussinesq's Solutions

As a preliminary exercise a comparison will be made between the integrated Mindlin's solution developed previously and integrated forms of Boussinesq's equation for the same parameter encountered in the literature.

Mindlin's solution is developed exclusively for sub-surface loading, this section looks at the effectiveness of Mindlin's solution if the value of c were reduced to 0 as to imply the loading is at the surface. Furthermore this exercise will validate whether or not Mindlin's solution has been correctly integrated in Eq. 4.12.

Take $c = 0$ m (so that the load acts at the surface) therefore,

$$m = 3(3-4\nu)z(z+c)^2 - 3c(z+c)(5z-c) = 3(3-4\nu)z(z)^2 - 0 = 3z^3(3-4\nu)$$

substituting these into Eq. 4.12 gives,

$$\sigma_z = -\frac{q}{4-4\nu}\left[\left[\frac{z(1-2\nu)}{\sqrt{R^2+z^2}}\right] - \left[\frac{z(1-2\nu)}{\sqrt{R^2+z^2}}\right] + \left[\frac{z(1-2\nu)}{\sqrt{z^2}}\right] - \left[\frac{z(1-2\nu)}{\sqrt{z^2}}\right] + \left[\frac{z^3}{\sqrt{R^2+z^2}^3}\right] - \left[\frac{z^3}{\sqrt{z^2}^3}\right] + \left[\frac{3z^3(3-4\nu)}{3\sqrt{R^2+z^2}^3}\right] - \left[\frac{3z^3(3-4\nu)}{3\sqrt{z^2}^3}\right] + 0\right]$$

$$\sigma_z = -\frac{q}{4-4\nu}\left[\left[\frac{z^3}{\sqrt{R^2+z^2}^3}\right] - 1 + \left[\frac{z^3(3-4\nu)}{\sqrt{R^2+z^2}^3}\right] - (3-4\nu)\right]$$

$$\sigma_z = -\frac{q}{4-4\nu}\left[\left[\frac{z^3}{\sqrt{R^2+z^2}^3}\right] + \left[\frac{z^3(3-4\nu)}{\sqrt{R^2+z^2}^3}\right] - (4-4\nu)\right]$$

$$\sigma_z = -\frac{q}{4-4\nu}\left[\frac{z^3(4-4\nu)}{(R^2+z^2)^{3/2}} - (4-4\nu)\right]$$

$$\sigma_z = \frac{q(4-4\nu)}{(4-4\nu)} - \frac{qz^3(4-4\nu)}{(4-4\nu)(R^2+z^2)^{3/2}}$$

$$\sigma_z = q\left(1 - \frac{z^3}{(R^2+z^2)^{3/2}}\right) \tag{4.13}$$

From Dominguez (1966) the integrated version of Boussinesq's equation for σ_z is.

$$\sigma_z = q\left[1 - \frac{z^3}{(R^2+z^2)^{3/2}}\right]$$

The two solutions are identical which confirms that Mindlin's solution has been correctly integrated (Eq. 4.12).

Chapter 5

Exploring the Applications of the Integrated Mindlin's Solution

This section explores some possible applications for the integrated Mindlin's solution developed earlier (Eq. 4.12).

5.1 Mindlin Based Influence Chart

A Mindlin-based influence chart would offer advantages such as quick approximation, the ability to obtain values for irregular shaped loadings and easier calculation of stresses that are offset (do not lie directly beneath the center of the circular loading). Such charts do not appear to exist for Mindlin's solution though have been developed for Boussinessq's solution, namely Newmark's chart developed by Nathan Newmark in 1942 (Das & Sobhan 2010).

Noting the likeness between the integrated Mindlin's solution (Eq. 4.12) and the integrated Boussinesq's solution for normal stress induced by a vertical load an at-

tempt was made to develop an influence chart for Mindlin's solution similar to that of Newmark's influence chart for Boussinesq's solution. Newmark's influence chart is of great practical value due to its versatility, efficiency and useful approximation capabilities.

In order to develop a chart similar to that of Newmark's several variables had to be taken as constants, namely, poisson's ratio ν and the ratio c/z, where c is the depth from the surface to the loaded area and z is the depth of the point of interest. If these constants were taken as variables the values used to generate the chart would not correlate and the chart would be useless. A trial and error approach was undertaken by inputting different values of R into Eq. 4.12 to obtain predetermined incremental values of $\frac{\sigma_z}{q}$. The same inputs used to generate Newmark's chart were targeted. Figure 5.1 shows the table of these results for $c/z = 0.3$ and $\nu = 0.3$. Newmark's chart represents a special case of these charts with $c/z = 0$.

For c /z = 0.3			
sigma/q	R/z	sigma/q	R/z
0	0	0.55	0.7605
0.05	0.164	0.6	0.8338
0.1	0.238	0.65	0.9162
0.15	0.2996	0.7	1.011
0.2	0.356	0.75	1.1226
0.25	0.41	0.8	1.262
0.3	0.4635	0.85	1.446
0.35	0.5176	0.9	1.72
0.4	0.5734	0.95	2.2478
0.45	0.6316	1	∞
0.5	0.694		

Figure 5.1: Table of values for creation of Newmark style Mindlin based influence chart. $c/z = 0.3$ and ν=0.3.

Like in Newmark's chart values of R/z were then used as the radii for the circles in Figure 5.2. Again like Newmark's chart the circles are dissected by evenly spaced angular lines, the influence value is obtained by $1/N$, where N is the number of elements on the chart and the length of line AB represents the unit length

$R/z = 1$(Das & Sobhan 2010).

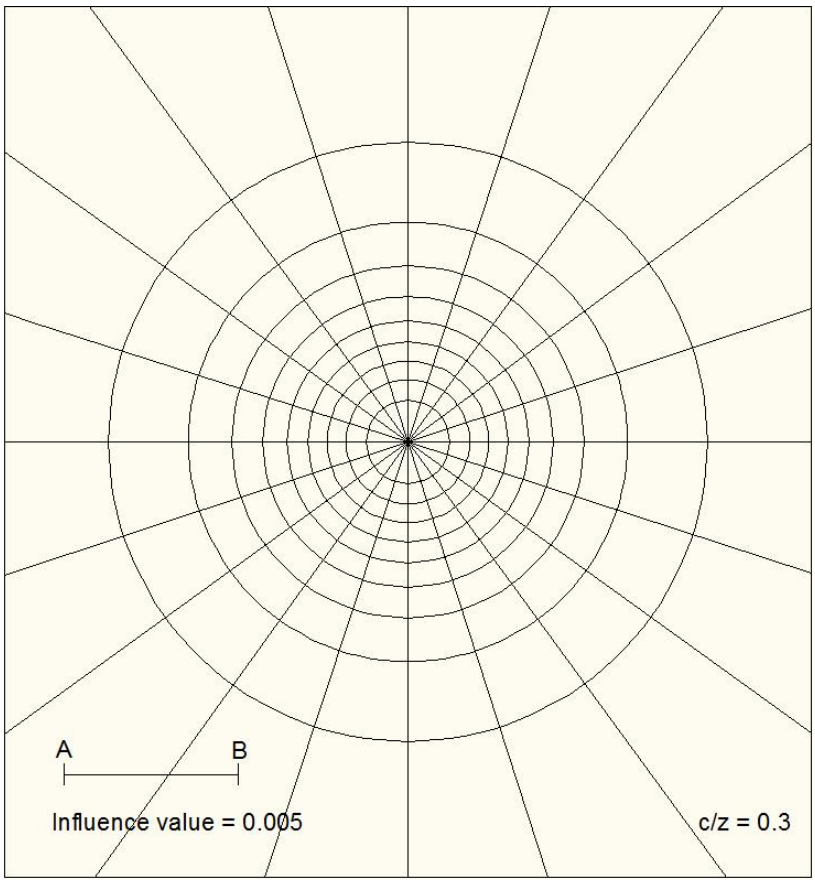

Figure 5.2: The developed Mindlin based influence chart for $c/z = 0.3$ and $\nu = 0.3$.

Two tests were performed to validate the accuracy of Figure 5.2 using the same equation as Newmark's chart (Das & Sobhan 2010, pp.344).

$$\sigma_z = (IV)qM \tag{5.1}$$

where, IV is the influence value, q is the area load and M is the number of elements covered by the area when placed on the chart. The diagrammatic components of the following tests are located in Appendix B.

TEST 1

$z = 10\text{m}$

$c = 3\text{m}$

$R = 5\text{m}$

$q = 150\text{kN}$

which gives 66 elements on chart therefore,

$\sigma_z = 0.005 \cdot 66 \cdot 150 = 49.5 \text{ kN/m}^2$

The above values when substitued into Mindlin's solution gives $\sigma_z = 50.08 \text{ kN/m}^2$

$error = 1.158\%$

Therefore, a good agreement was found and the chart can be deemed accurate.

TEST 2

$z = 8\text{m}$

$c = 3\text{m}$

$R = 2\text{m}$

$q = 150\text{kN}$

which gives 23 elements on chart therefore,

$\sigma_z = 0.005 \cdot 23 \cdot 150 = 17.25 \text{ kN/m}^2$

The above values when substituted into Mindlin's solution gives $\sigma_z = 18.04 \text{ kN/m}^2$

$error = 4.38\%$ This error is much higher than test 1, which shows the chart not useful for $\frac{c}{z} \neq 0.3$

5.1.1 Limitations

Although this chart can provide a quick and accurate approximation, the concept of a Mindlin's solution-based influence chart is of little practical value overall due to the many variables which must maintain a constant value for the chart to be produced. Therefore a different chart must be produced depending on different values of c/z and ν. Further simplification was investigated with the aim to achieve a pair of charts or graphs with one similar to Figure 5.2 and another that would give a different scale to be utilised in conjunction with the other based off of ν and $\frac{c}{z}$. However due to the complexity of the integrated Mindlin's solution (Eq. 4.12), this task was deemed too difficult to achieve with questions over its general possibility.

Therefore even though a Mindlin-based influence chart was successfully created, it serves little practical value due to the need to generate a great number of charts for a great number of situations which would be very time consuming.

5.2 Stress Estimation In Bi-Loaded Anchors

Having reached severe limitations with the Mindlin based influence chart in the previous section the need to find an useful application for Eq. 4.12 remained. Investigations into applications for which the circular subsurface loading equation could be applied were undertaken with a preference that it have practical relativity. It was decided that the solution could obtain useful results if applied to a simplified anchor system. Recognition that both Boussinesq's and Mindlin's solutions are mathematically compatible and therefore combinationally possible, provided a particular avenue of intrigue. A bi-loaded anchor system, one of which that contained two loads, a surface load representable by Boussinesq's solution, and a subsurface load expressible by that of Mindlin's solution was explored.

It was deemed that Eq. 4.12 may be an effective way to determine the amount of loading required to eliminate tension in bi-loaded ground anchors. Figure 5.3 shows the loading conditions for a bi-loaded ground anchor analysed in this thesis. Such an anchor is commonly used in practice as the compressive force applied at the surface further strengthens the anchorage. Given a uniformly distributed circular surface and sub-surface load it is possible to then combine both Eqs. 4.12 and 4.13 (Mindlin's and Boussinesq's respectively) to formulate what surface loading is required to nullify tensile stresses directly beneath the sub-surface load. It is an important area of examination with practical significance as tensile stresses in soil beneath the ground anchor would ultimately mean failure due to the poor tensile capacity of soil.

Both Boussinesq's and Mindlin's solutions are particularly compatible in this circumstance as the value of z would be the same for both. As a negative stress indicates a tensile stress, combining Eqs. 4.12 and 4.13, equating to zero and then solving for the circular surface load would give the load needed at the surface to nullify tensile stresses beneath the anchor.

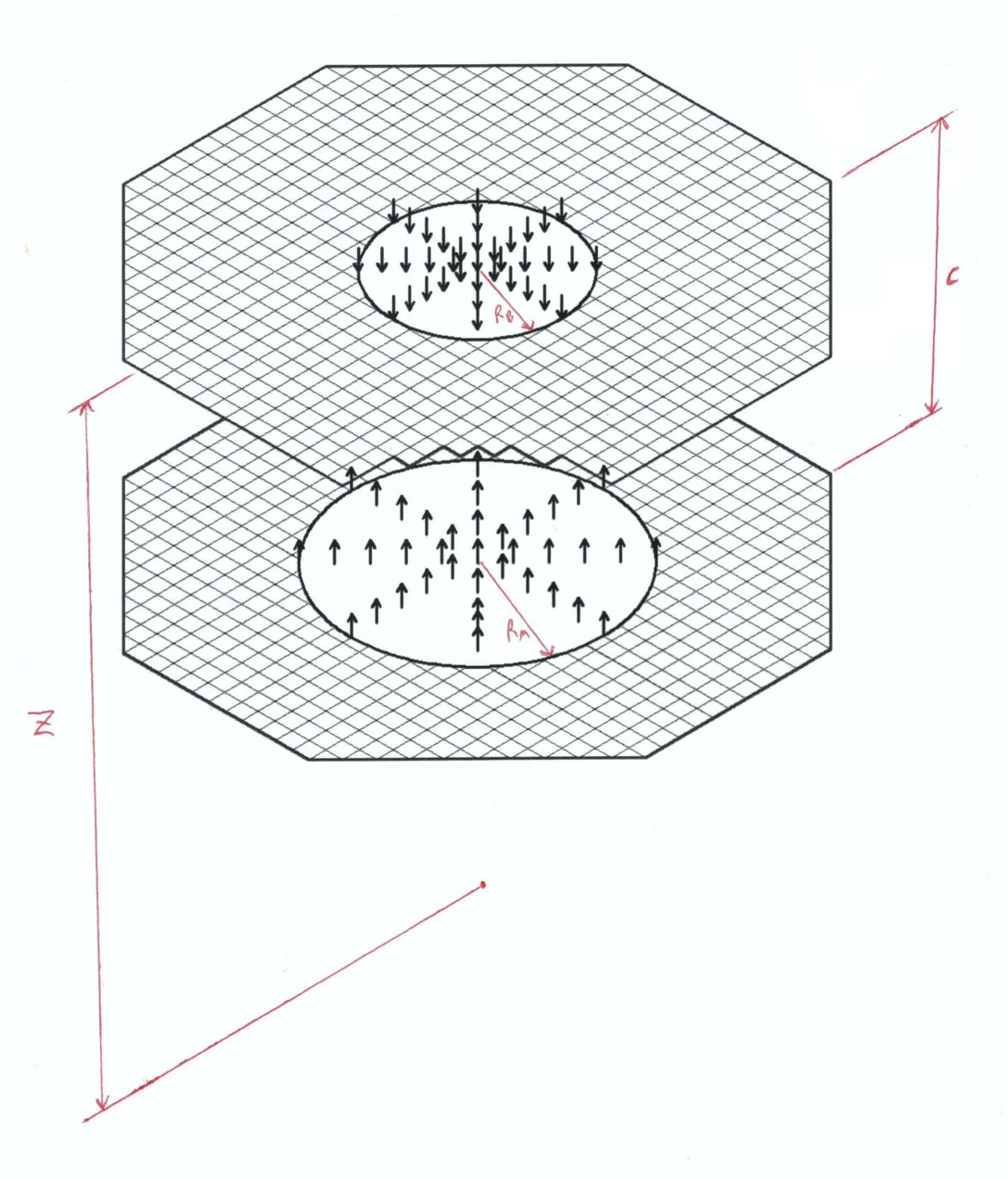

Figure 5.3: An isometric representation of a bi-loaded anchor system with a Boussinesq load acting on the surface plane and a Mindlin load acting on a parallel sub-surface plane a distance of c below.

5.2.1 Example

This example displays the steps involved in finding the required q_B to nullify tensile stresses, although as seen in the next section this is not the penultimate solution in doing so.

Taking $z = c$ as this is where the maximum tensile stresses would reside.

$\nu = 0.25$

$z = c = 5\text{m}$

$R_B = 1.2\text{m}$

$R_M = 1.2\text{m}$

$q_M = 200\ \text{kN/m}^2$

$\text{q}_B = ?$

Taking the integrated Mindlin solution

$$\begin{aligned}\sigma_z = -\frac{q_M}{4-4\nu}\Bigg[&\left[\frac{(1-2\nu)(z-c)}{\sqrt{R_M^2+(z-c)^2}}\right]-\left[\frac{(1-2\nu)(z-c)}{\sqrt{(z-c)^2}}\right]-\left[\frac{(1-2\nu)(z-c)}{\sqrt{R_M^2+(z+c)^2}}\right]\\&+\left[\frac{(1-2\nu)(z-c)}{\sqrt{(z+c)^2}}\right]+\left[\frac{(z-c)^3}{\sqrt{R_M^2+(z-c)^{2^3}}}\right]-\left[\frac{(z-c)^3}{\sqrt{(z-c)^{2^3}}}\right]\\&+\left[\frac{m}{3\sqrt{R_M^2+(z+c)^{2^3}}}\right]-\left[\frac{m}{3\sqrt{(z+c)^{2^3}}}\right]+\left[\frac{6cz(z+c)^3}{\sqrt{R_M^2+(z+c)^{2^5}}}\right]-\left[\frac{6cz(z+c)^3}{\sqrt{(z+c)^{2^5}}}\right]\Bigg]\end{aligned}$$

where

$$m = 3(3-4\nu)z(z+c)^2 - 3c(z+c)(5z-c)$$

and the integrated Boussinesq solution

$$\sigma_z = q_B\left[1-\frac{z^3}{(R_B^2+z^2)^{3/2}}\right]$$

substituting in the values we get

$$m = 3(3 - 4 \times 0.25)5(5+5)^2 - 3 \times 5(5+5)(5 \times 5 - 5) = 3000 - 3000 = 0$$

$$q_B \left[1 - \frac{5^3}{(0.8^2 + 5^2)^{3/2}}\right] = \frac{200}{4 - 4 \times 0.25} \left[\left[-(1 - 2 \times 0.25) - 1 + \left[\frac{6 \times 5 \times 5(5+5)^3}{\sqrt{1.2^2 + (5+5)^2}^5}\right]\right.\right.$$
$$\left.\left. - \left[\frac{6 \times 5 \times 5(5+5)^3}{\sqrt{(5+5)^2}^5}\right]\right]$$

$$0.08057 q_B = 66.6667 \left[-0.5 - 1 + 1.4473 - 1.5\right]$$

$$0.08057 q_B = 66.6667 \times -1.5527$$

$$q_B = \frac{-103.5133}{0.08057}$$

$$q_B = -1284.8 kN/m^2$$

5.2.2 Graphical Approach for a Bi-Loaded Anchor System

Having reached difficulties in developing an effective Newmark style influence chart for Mindlin's solution, an attempt was made to create a graph which was also based on influence factors (σ_z/q) that could allow an easy comparison between integrated Mindlin's and Boussinesq's solutions. The plots in this section were developed using the computer program MATLAB, the code for which can be found in Appendix C. Figure 5.4 shows the influence factor curves for multiple values of ν and for Boussinesq's equation for an increasing ratio R/z.

Discussion of Figures 5.4, 5.5 and 5.6

An interesting thing to note is that when $z = c$ and $R = 0$, the integrated Mindlin's solution is equal to $\frac{1}{2}$. This emulates what happens when c approaches ∞ where Mindlin's solution becomes reminiscent Kelvin's solution. Figure 5.4 can be used for estimating the R/z required for the Boussinesq load to nullify the maximum

tensile stresses caused by the subsurface Mindlin load (which is at the point of loading $z = c$). The figure also conveys a strange result, the curves for $\nu = 0.5$ and $\nu = 0.4$ gives an $I > 1$ at a certain range of R/z with a maximum of 1.009 occurring at $R/z = 4$ on the $\nu = 0.5$ curve. Such a result should be impossible as the maximum difference between compressive and tensile influence factors should be exactly equal to 1 at $z = c$. The point located infinitesimally above c^+, should emanate a compressive stress and the point infinitesimally below c^-, a tensile stress given the load is acting directly upwards, normal to the surface. An influence factor of > 1 negates such a necessity. The cause of this anomaly is unknown but it could represent a problem or limitation of Mindlin's solution.

Following the curve for $\nu = 0.5$, when $R/z = 1$ the influence factor is 0.75 and from the Boussinesq curve, the surface loading would require an $R/z = 1.233$ to achieve the same influence factor and counter this. Therefore from this information we know that the R_B would need to be altered in Eq. 4.13, see below.

$$\sigma_z = q\left(1 - \frac{z^3}{((1.233R_B)^2 + z^2)^{3/2}}\right)$$

Doing so, arrives at Figure 5.6 which indicates that tensile stresses are still present. An explanation for this presence can be obtained by observing Figure 5.5 which exhibits the decline in stress caused by both loads as the depth increases. This element is a limitation of Figure 5.4 as it does not take into account the weakening intensity of the Boussinesq surface load as the depth z, increases. So the above equation results in Figure 5.6 where tensile stresses are nullified at the point of loading ($\sigma_z = 0$ at c^-) but as the depth z, increases below this point there is a zone where the subsurface Mindlin loading has much more of an influence on the stress conditions than Boussinesq's surface load does and hence tensile stresses remain. It is possible to develop a graphical relationship between the surface and subsurface loadings that nullify not only the maximum, but *all* tensile stresses, this is presented in the next section.

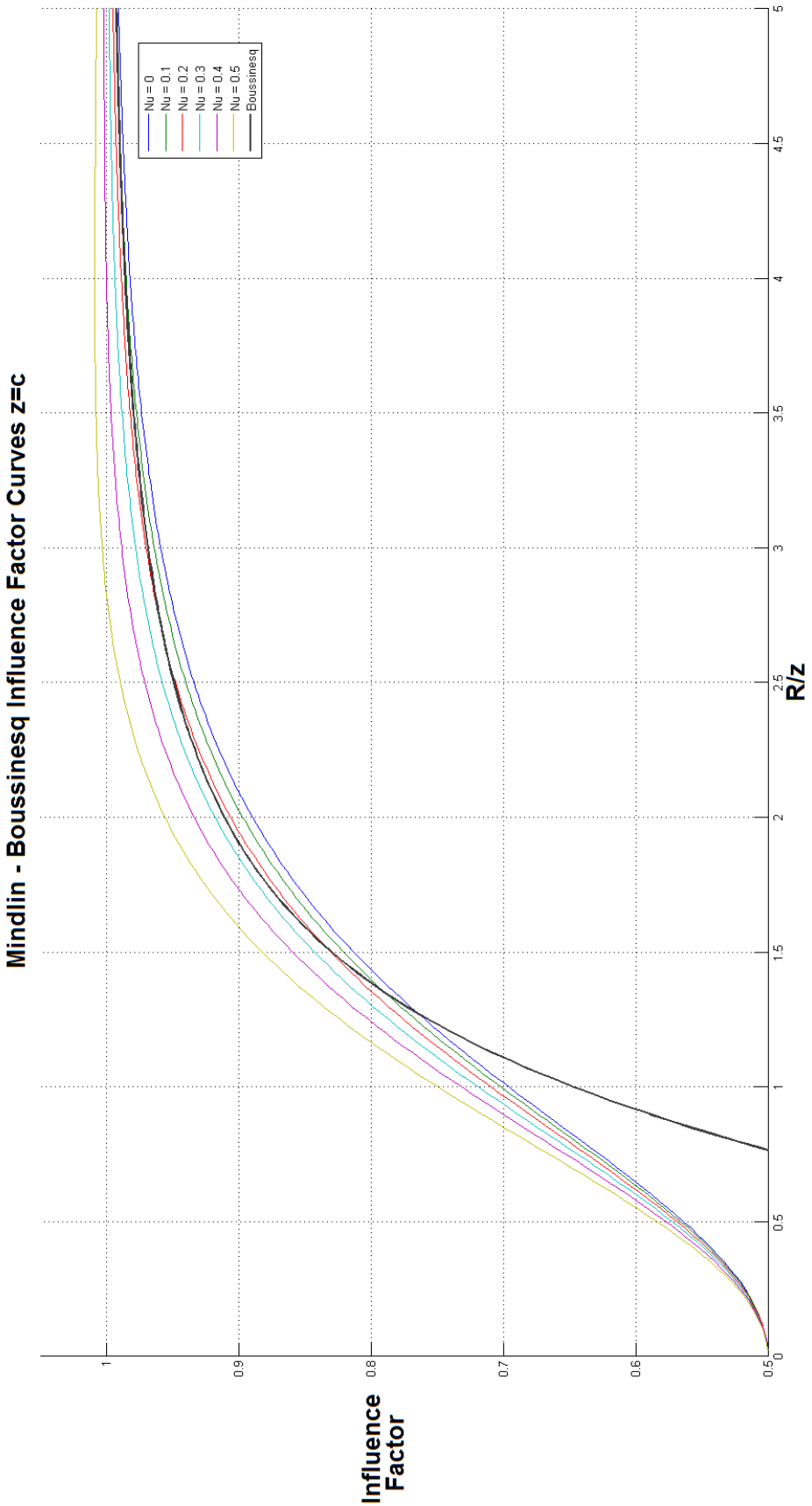

Figure 5.4: Influence factor curves for eq. 4.12 with $\nu = 0, 0.1, ...0.5$ and eq. 4.13.

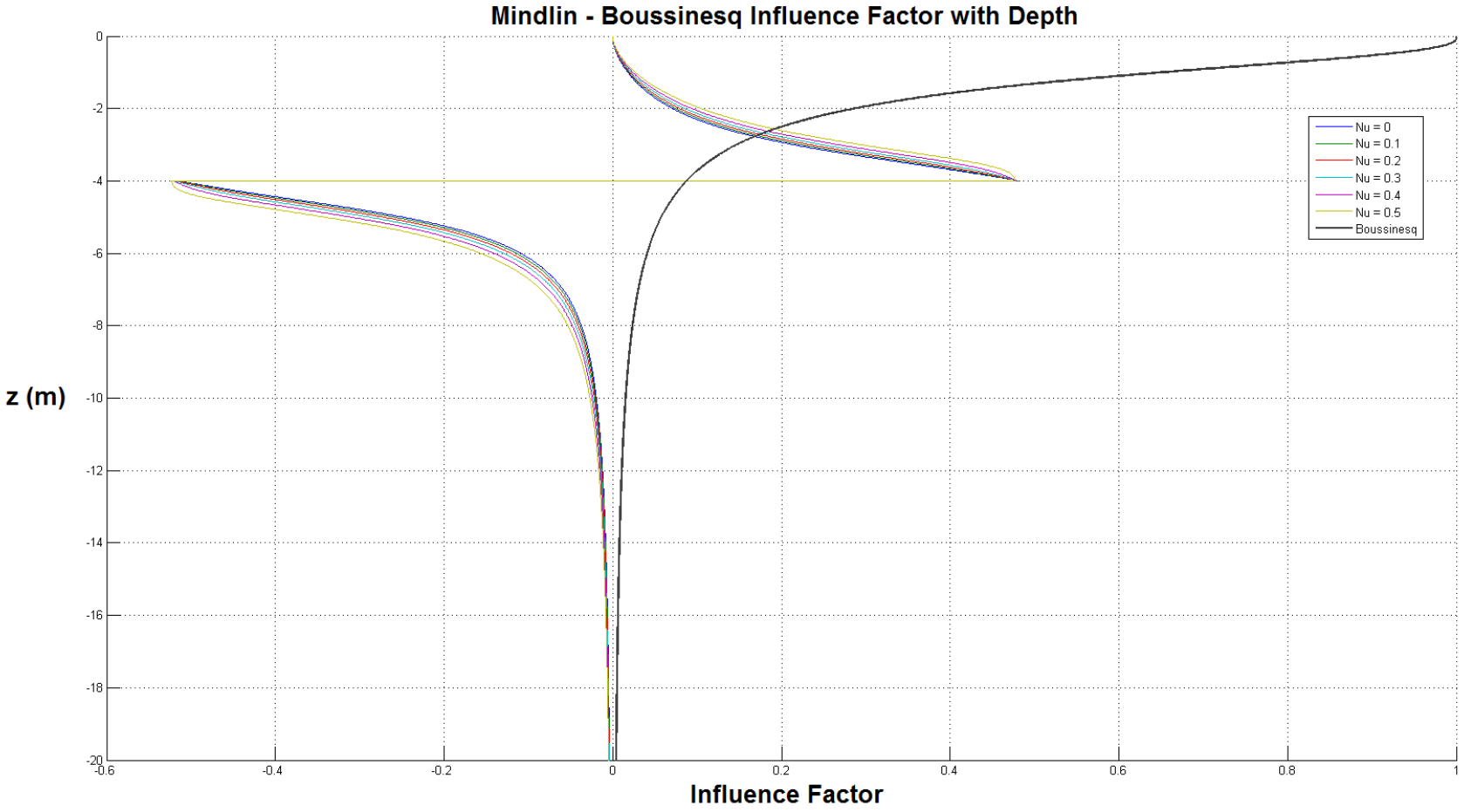

Figure 5.5: Behaviour of influence factor curves for eq. 4.12

(where $\nu = 0$, 0.1,...0.5) and eq. 4.13 against increasing depth z. $c = 4$m.

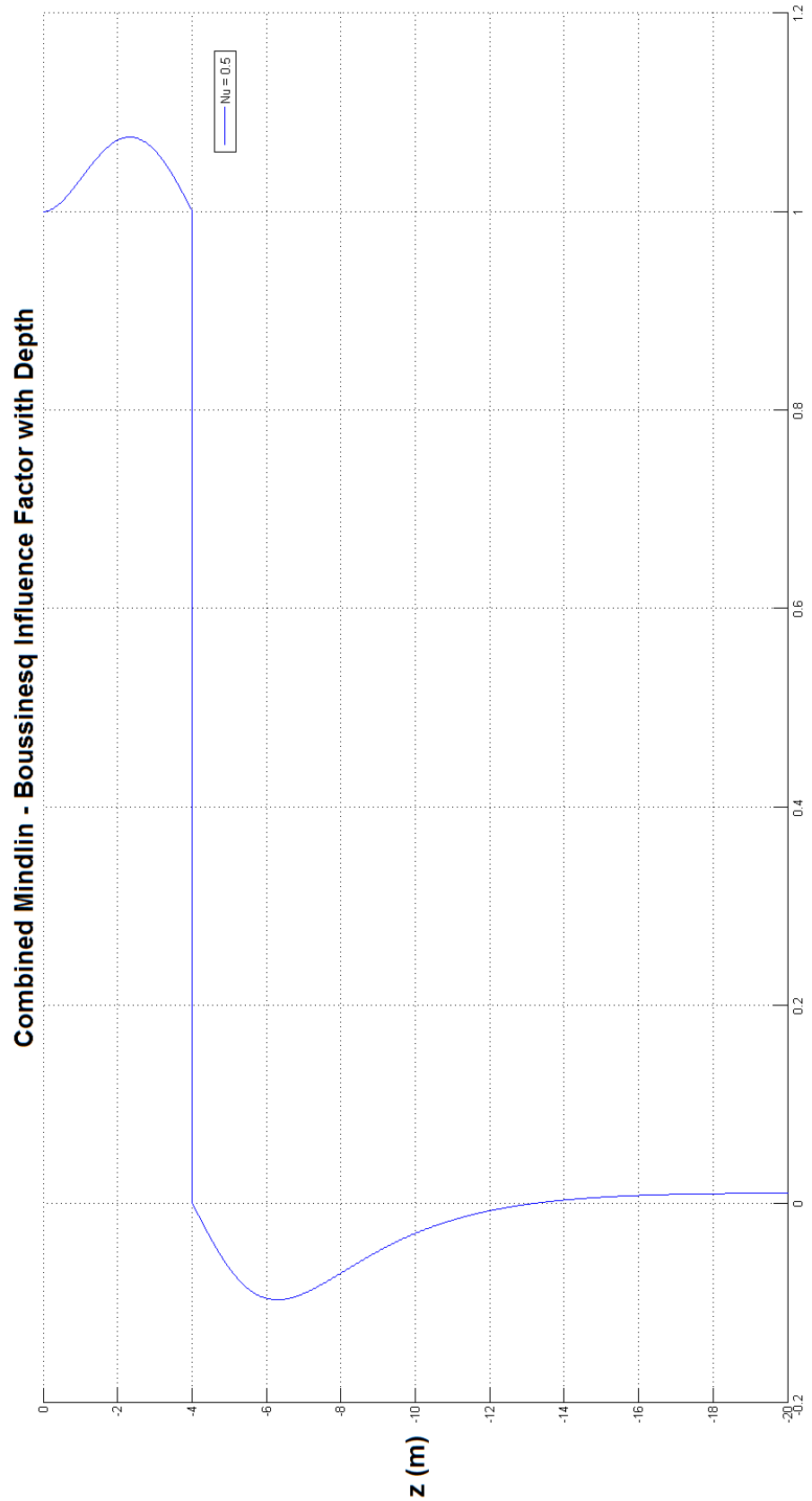

Figure 5.6: Behaviour of a combined Mindlin - Boussinesq influence factor curve against increasing depth z. $c = 4$m.

5.2.3 Cancelling All Tensile Stresses

Following on from Figures 5.5 and 5.6 where we have $c = 4\text{m}$, $R_B = R_M = R = 4\text{m}$ and $\nu = 0.5$ this section shows the development of an equation which gives the maximum required ratio of q_B/q_M so that no tensile stress regions will appear in the ground. Taking the integrated forms of Mindlin's and Boussinesq's equations (Eqs. 4.12 and 4.13 respectively) and equating them to one another ensures that the stress should be exactly neutralized for any specific depth $z(\text{m})$ (provided their loads are acting in opposite directions).

$$
\begin{aligned}
q_B\left[1-\frac{z^3}{(R^2+z^2)^{3/2}}\right] = &-\frac{q_M}{4-4\nu}\left[\left[\frac{(1-2\nu)(z-c)}{\sqrt{R^2+(z-c)^2}}\right]-\left[\frac{(1-2\nu)(z-c)}{\sqrt{(z-c)^2}}\right]\right.\\
&-\left[\frac{(1-2\nu)(z-c)}{\sqrt{R^2+(z+c)^2}}\right]+\left[\frac{(1-2\nu)(z-c)}{\sqrt{(z+c)^2}}\right]\\
&+\left[\frac{(z-c)^3}{\sqrt{R^2+(z-c)^2{}^3}}\right]-\left[\frac{(z-c)^3}{\sqrt{(z-c)^2{}^3}}\right]+\left[\frac{m}{3\sqrt{R^2+(z+c)^2{}^3}}\right]\\
&\left.-\left[\frac{m}{3\sqrt{(z+c)^2{}^3}}\right]+\left[\frac{6cz(z+c)^3}{\sqrt{R^2+(z+c)^2{}^5}}\right]-\left[\frac{6cz(z+c)^3}{\sqrt{(z+c)^2{}^5}}\right]\right]
\end{aligned}
$$

$$
\begin{aligned}
\frac{q_B}{q_M} = &-\frac{1}{4-4\nu}\left[\left[\frac{(1-2\nu)(z-c)}{\sqrt{R^2+(z-c)^2}}\right]-\left[\frac{(1-2\nu)(z-c)}{\sqrt{(z-c)^2}}\right]-\left[\frac{(1-2\nu)(z-c)}{\sqrt{R^2+(z+c)^2}}\right]\right.\\
&+\left[\frac{(1-2\nu)(z-c)}{\sqrt{(z+c)^2}}\right]+\left[\frac{(z-c)^3}{\sqrt{R^2+(z-c)^2{}^3}}\right]-\left[\frac{(z-c)^3}{\sqrt{(z-c)^2{}^3}}\right]\\
&+\left[\frac{m}{3\sqrt{R^2+(z+c)^2{}^3}}\right]-\left[\frac{m}{3\sqrt{(z+c)^2{}^3}}\right]+\left[\frac{6cz(z+c)^3}{\sqrt{R^2+(z+c)^2{}^5}}\right]\\
&\left.-\left[\frac{6cz(z+c)^3}{\sqrt{(z+c)^2{}^5}}\right]\right]\cdot\left[1-\frac{z^3}{(R^2+z^2)^{3/2}}\right]^{-1}
\end{aligned}
\tag{5.2}
$$

Using this equation for an array of z values gives Figure 5.7. Note that the peak negative influence factor on Figure 5.6 occurs at a depth of 6.28m which does not equal where the peak ratio is situated in Figure 5.7 which occurs at 7.9m. This makes sense because again, Boussinesq's equation is continually getting less intense. Figure 5.8 is proof that implementing the ratio $q_B/q_M = 1.593$ obtained from Figure 5.7 into the equation below eliminates all tensile stresses in the system.

$$I = I_M + (\frac{q_B}{q_M})I_B$$

where,

I_M is the Mindlin influence factor (σ_M/q_M)
I_B is the Boussinesq influence factor (σ_B/q_B)

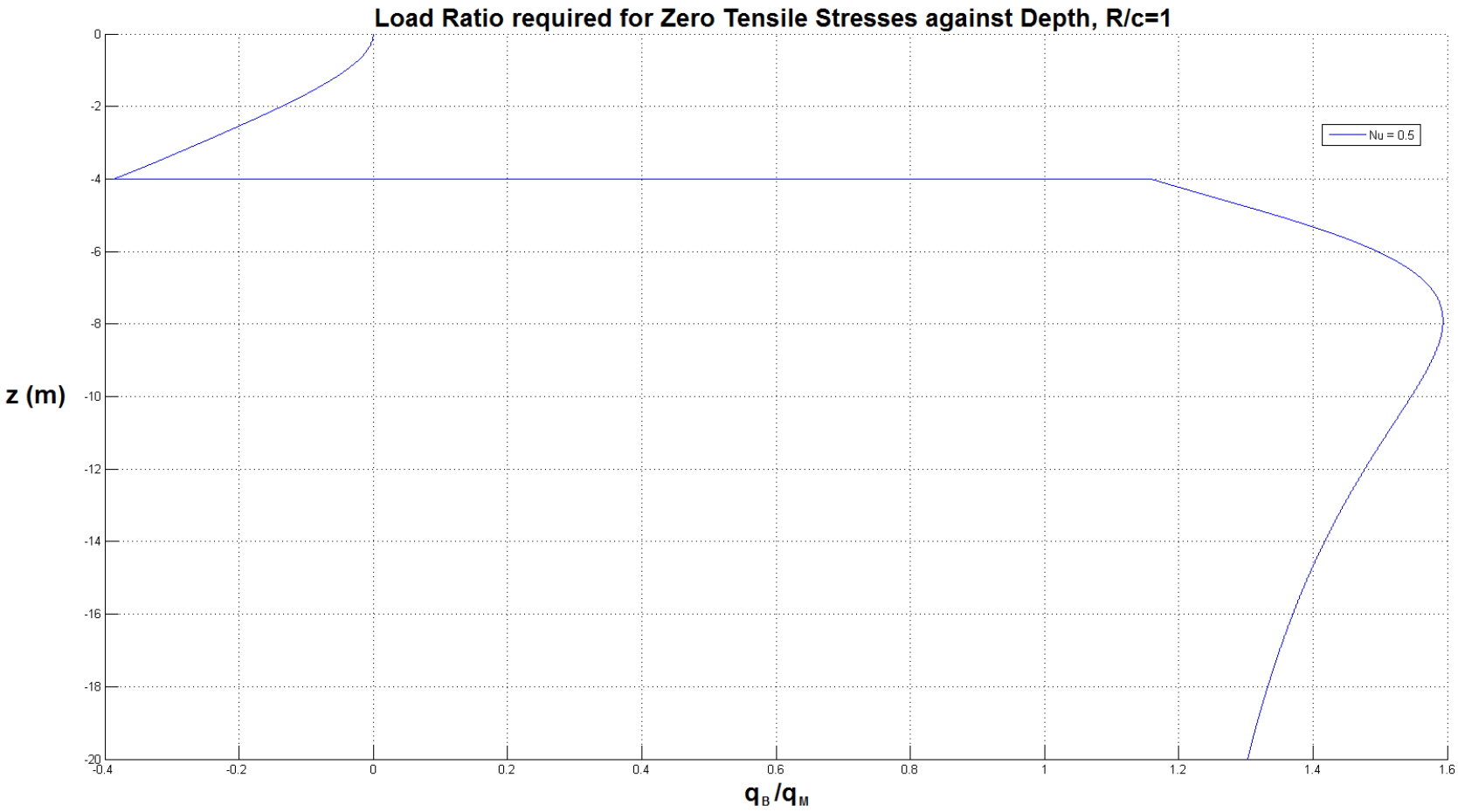

Figure 5.7: Ratio of loads required to nullify tensile stresses at depth z. $c = 4\text{m}$, $R = 4\text{m}$.

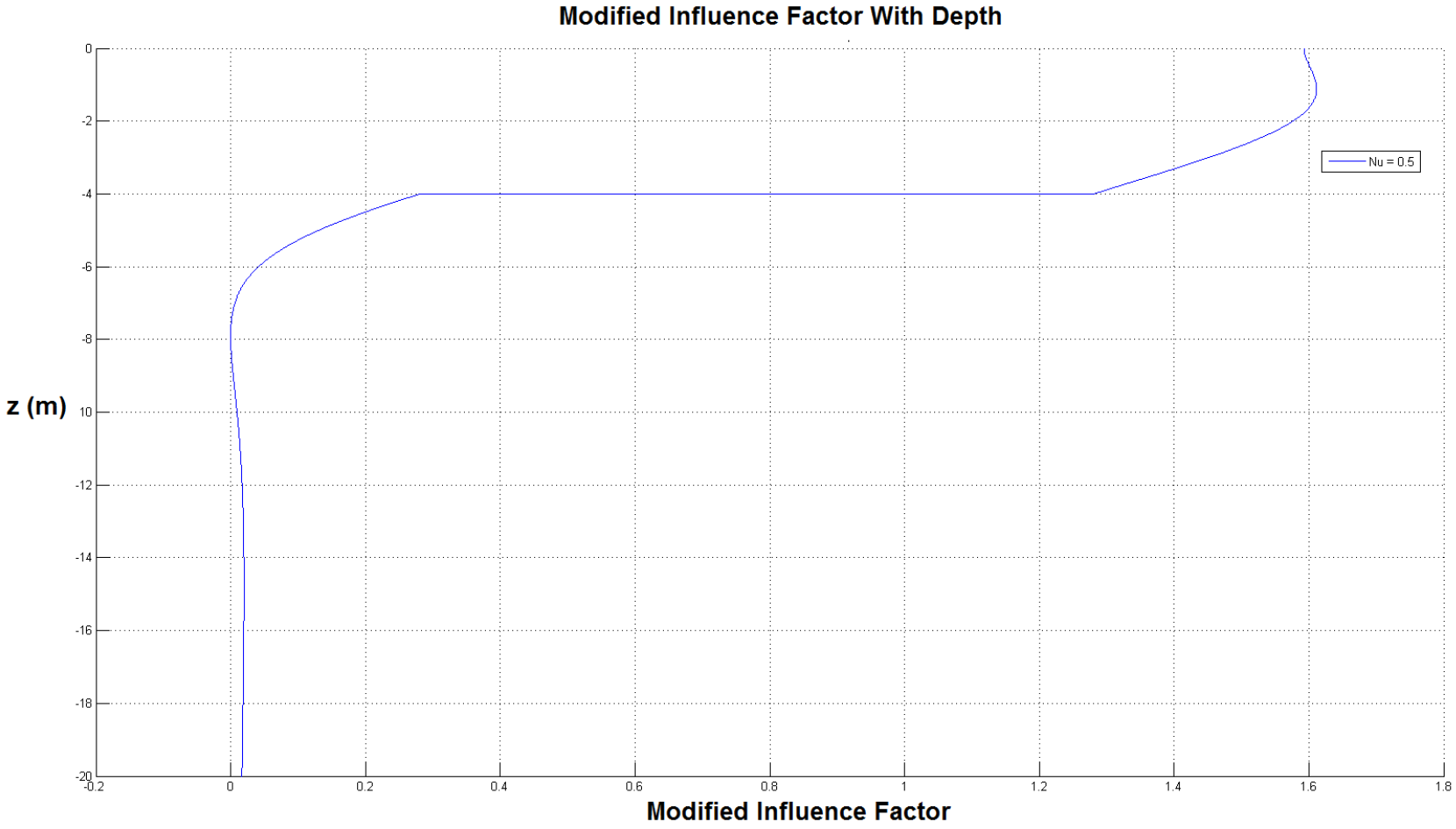

Figure 5.8: Modified to include q_B/q_M ratio from Figure 5.7, the combined Mindlin - Boussinesq influence factor curve against increasing depth z. $c = 4$m, $R = 4$m.

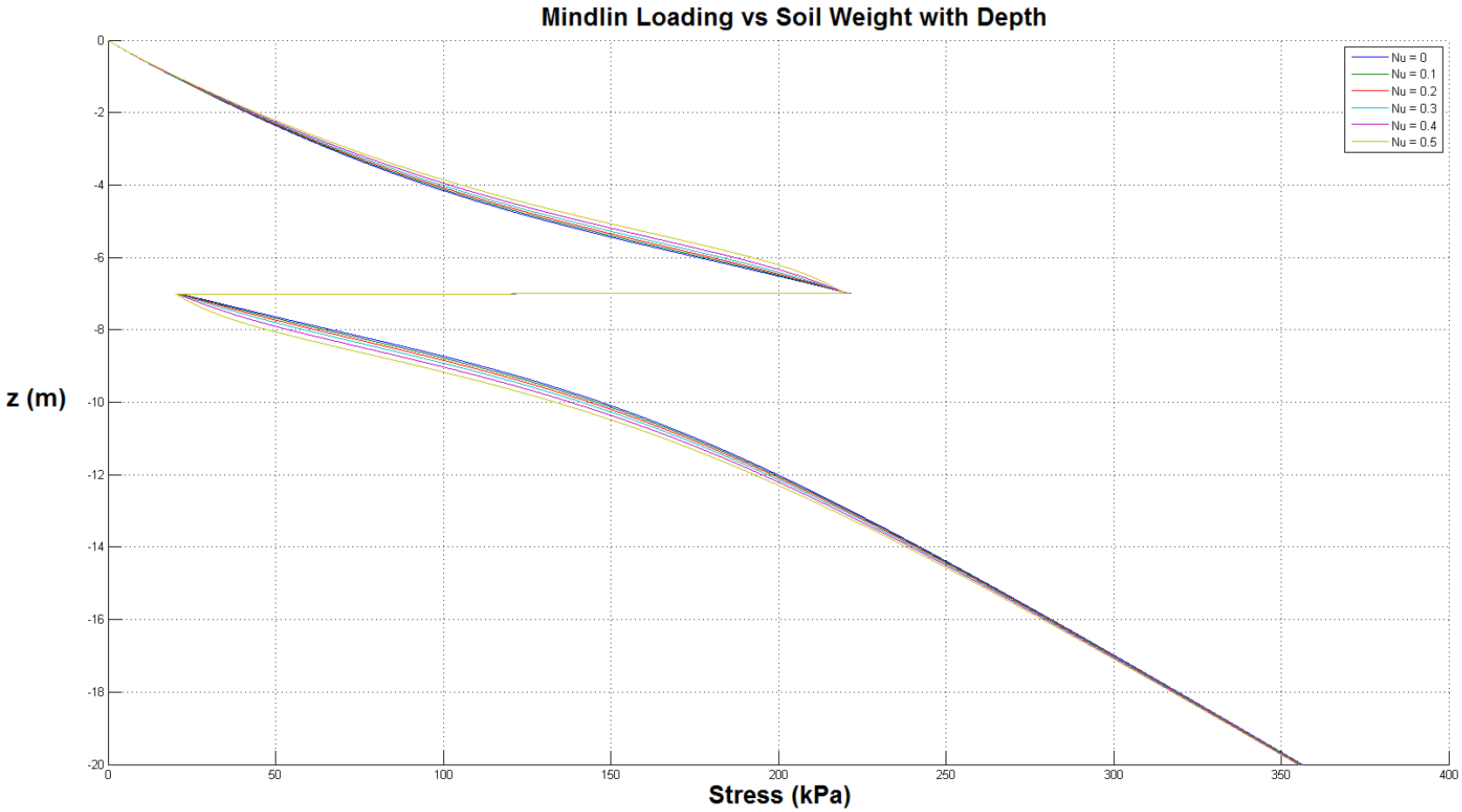

Figure 5.9: Stress with depth, no surface load $c = 7\text{m}$, $R = 2\text{m}$, $q = 200\text{kPa}$ and $\gamma = 18\text{kN/m}^3$.

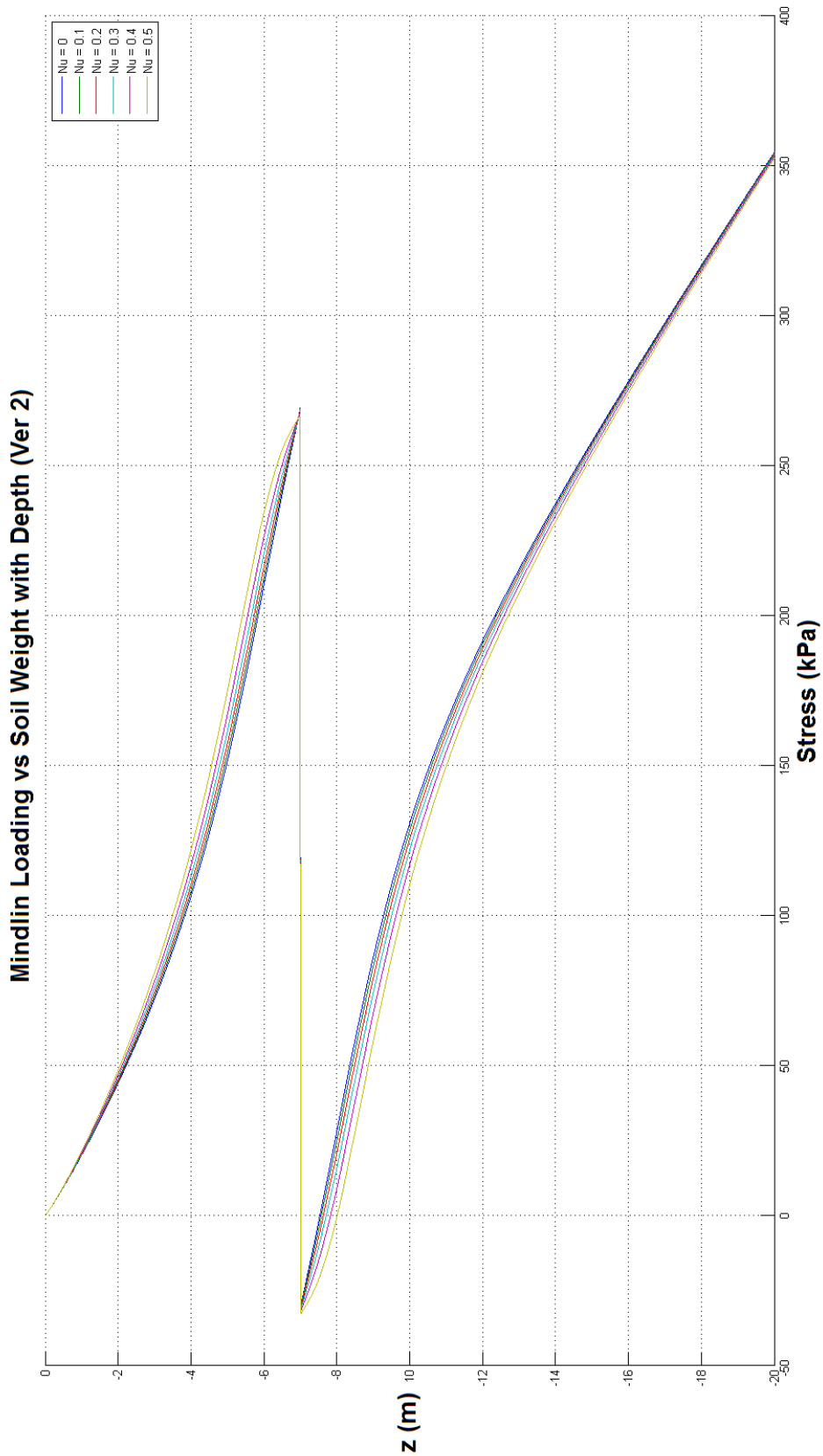

Figure 5.10: Stress with depth, no surface load $c = 7\text{m}$, $R = 2\text{m}$, $q = 300\text{kPa}$ and $\gamma = 18\text{kN/m}^3$.

Discussion of Figures 5.9 and 5.10

Figures 5.9 and 5.10 show the stress against depth when instead of a surface load, the uplift force of the anchor is mitigated purely by the weight of the soil, γ (kN/m^3). The difference that can be observed between Figure 5.9 and Figure 5.10 is a demonstration of the ability and ease of which a parametric study can be performed with these solutions. Figure 5.9 would indicate that the weight of the soil is enough to ensure the anchor system is entirely in compression and therefore would not fail, whereas figure 5.10 illustrates that increasing the Mindlin load from 200kPa to 300kPa and not changing any of the other variables would induce tensile stresses and therefore possible soil failure for this particular case.

Summary

Similarly to the Mindlin based influence chart developed earlier, the figures up until this point require numerical inputs for some parameters which limits their practical value. Specific values of c, R and additionally in the second case, q and γ must be chosen before the graphs can be generated. Although unlike the Newmark styled influence chart from earlier, the figures created represent a visual and insightful demonstration of how stress weakens with depth as well as the entanglement of Boussinesq's and Mindlin's solutions and the overall influences that certain parameters have within them.

5.2.4 Forming a Single Design Chart

As the value of q_B/q_M required to nullify tensile stresses depends entirely on R/c (if both subsurface and surface loads have the same radius R, ie. $R_B = R_M = R$) a table of values could be formulated giving the maximum ratio of q_B/q_M for each R/c and from that, a graph. Given the complexity of Eq. 5.2, it is not possible to directly equate q_B/q_M to R/c so another method must be used. This would

be a very time consuming task to do manually but the computational power of MATLAB supplies a timely alternative. A major simplification in such a case would be that $R_B = R_M$ which, from a practical point of a view is not an overly demanding requirement. Furthermore, optimization of radii against surface and sub-surface loadings is possible with subsequent analysis.

Taking a look at Eq. 4.12 it can be seen that on the left hand side of the equation we have units of pressure denoted by σ_z and on the right hand side of the equation exterior to the main set of parentheses we also have a pressure given by q. Therefore the final unit obtained through solving for the terms inside the parentheses must be dimensionless. This allows that R, c and z to all be divided by c resulting in an identical dimensionless answer. Doing so allows the performance of computations with a unified variable R/c which is what is needed to determine maximum values of q_B/q_M. This approach was undertaken in the MATLAB code, giving Figure 5.11.

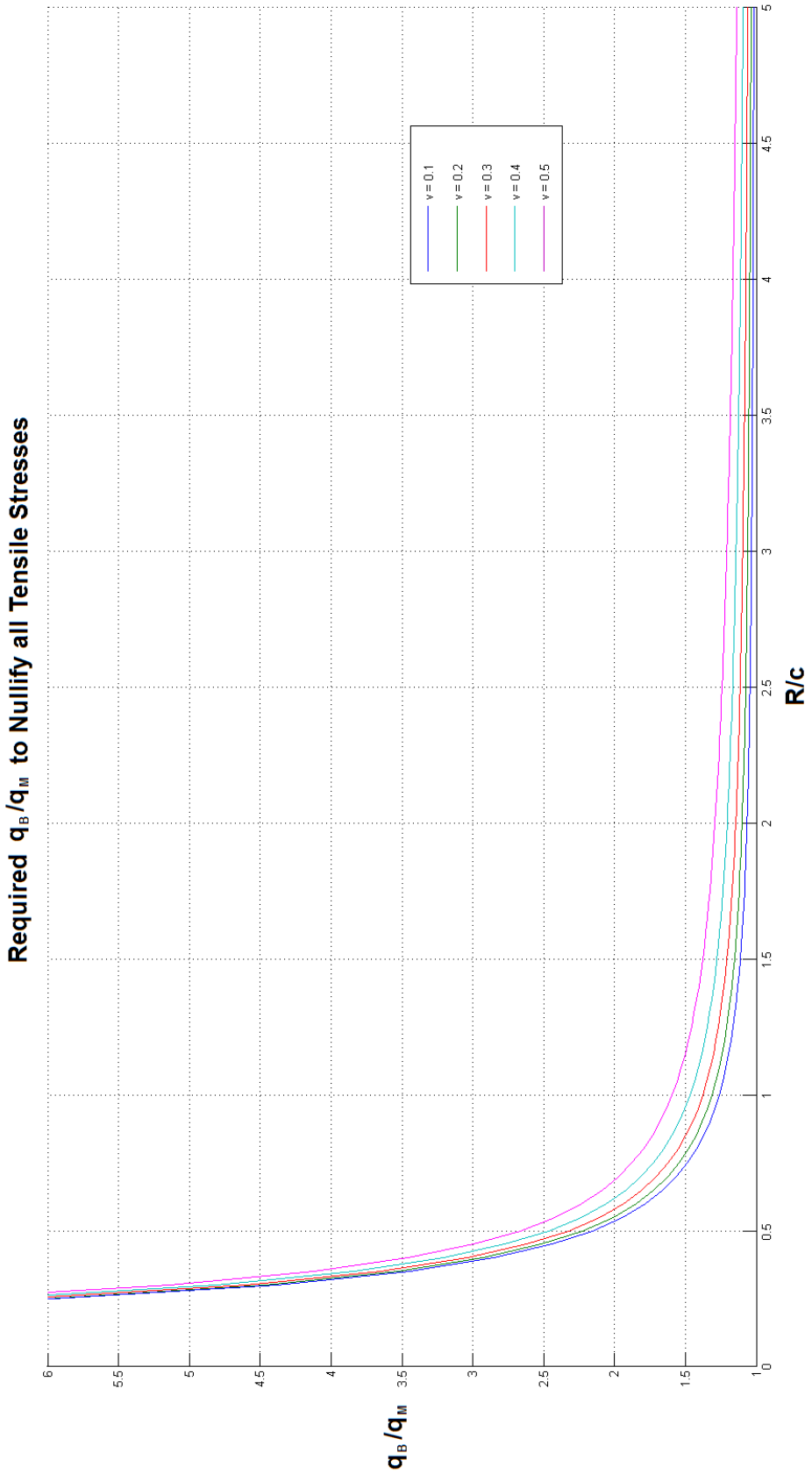

Figure 5.11: Design chart providing the required ratio of q_B/q_M for each value of R/c.

Figure 5.11 represents a design chart which, assuming that the radius of Boussinesq's load is equal to that of the Mindlin's load gives the required loading ratio on the surface against the subsurface to nullify all tensile stresses within the system. It was ensured that for each case, q_B/q_M achieved a maximum prior to reaching the limiting value of $z = 20$m used in the MATLAB script. It is also important to note that the chart does not take into account soil weight and thus it can be deemed as conservative.

5.2.5 Conclusion and Limitations

A single design chart (Figure 5.11) was reached, however it makes the assumption that $R_B = R_M$, which could be overcome by some further work on the solutions. The set back that was encountered of not fully taking into account the variation of stress intensity with depth was a great demonstration of the insight in which the closed form solution can give. The closed form nature means that the plots are exact and the graphical nature of the investigation allows for a quick visual inspection which is a useful educational tool. This section has also been an exhibition into the flexibility of the closed form solution and the ease at which modifications can be made.

Sabatini, Pass & Bachus (1999, pp. 68) state that when compression anchors (bi-loaded anchors) are to be used for permanent application, *pre-design test programs* may be required to assure satisfactory performance unless verification can be obtained from prior experience or research results. It would seem that the results (or similar) obtained from this thesis may be applicable to the aforementioned pre-design stage to suggest plausibility as it should give a conservative estimate. Although, it is likely that the results obtained here would need follow up work to make them more applicable for practical use.

It is important to stress however that although the figures in this section are focused on a practical topic, the anchor system analysed here is heavily simplified and thus the results gathered here are not entirely realistic. In addition to the aforementioned isotropic, homogeneous, elastic conditions of the soil media the model assumes that the anchor is flexible and that the loads on the anchor are uniformly distributed. It also neglects anchor thickness and for the bi-loaded case does not take into account soil weight. Anchors in practice are almost always angled, usually between 15 and 30 degrees (Sabatini, Pass & Bachus 1999, pp.70). The anchor in this problem and its associated mathematics are applicable only for an orientation normal to a horizontal surface. However an angled analysis would be possible by amalgamating multiple equations from Mindlin's solution for stresses in different directions.

Overall both benefits and limitations of the closed form solution can be readily seen throughout this section and a valid design chart was produced. Of further note the answer from the example performed in Section 5.2 was verified as correct using the MATLAB code. MATLAB code used for the creation of Figures 5.4 - 5.11 can be found in Appendix C.

Chapter 6

Conclusions and Further Work

6.1 Conclusions

Three related geotechnical, closed form solutions were chosen and researched. This research showed the applications for which they can be used; mainly, tunnelling, piling and anchoring. This research also gave an indication on the sorts of processes in which the solutions may be subjected to and just what could be achieved.

Mindlin's solution was successfully integrated for the vertical stress produced under the center of a circular sub-surface loading. This solution was used to obtain charts and plots that were compared and analysed. The first of which was a Newmark styled Mindlin based influence chart that was deemed not practically useful due to the fact that one chart would have to be produced for each configuration of variables. The next array of plots were based on an anchor system of which Figure 5.11 represents the final, and the most practical. It is capable of giving some conservative estimates in compression anchor design.

Of the main objectives outlined in the project specification (listed in Appendix

A), only the final and supplementary objective which was to compare the closed form solutions with their numerical alternatives was not undertaken due to time constraints.

On a whole the category of closed form solutions in geotechnical engineering was reviewed throughout this project; their prominent benefits were that of insight and flexibility and their main limitation, their simplifying assumptions.

6.2 Further Work

The mathematics for the anchor system that was investigated in Chapter 5 could be modified as to be more realistic. Most especially re-orientating the anchor at an angle and reducing a number of other unrealistic traits mentioned in Section 5.2.5.

In Section 5.2.3 an anchor system with no surface loading is examined and a small parametric study is performed but no singular design chart was developed that would show the depth required for an anchor to be placed so that purely the weight of the soil would nullify tensile stresses. Interest in to the prospect of a singular design chart for this case could be further investigated.

The reason for an $I > 1$ which is seen in Figure 5.4 is currently unknown. One possible reason for the anomaly is that it is a created as a result of the circular integration. If the same chart was generated for say, a rectangular integration the reason could be explained.

Comparisons with numerical solutions were not performed due to time limitations but would be a valuable source of information in certifying the overall value of closed form solutions in this area, and evaluate the levels of error caused by simplifying assumptions involved.

Kelvin's solution was chosen as one to be investigated in this project, but no results or data was obtained that was centred around it. One possible area of exploration would be the application of Kelvin's solution in deep tunnelling, where the effects of the surface could be deemed negligible.

References

Altun, S., Karakan, E., and Tuna, S. C. (2013). Load displacement relationship for a rigid circular foundation anchored by Mindlin soltuions. *Scientia Iranica*, 20(3):397–405.

Basile, F. (2002). Integrated form of singluar Mindlin's solution. In *Proc. 10th ACME Conference*, pages 191–194.

Bower, A. F. (2008). Analytical techniques and solutions for linear elastic solids. `http://solidmechanics.org/text/Chapter5_1/Chapter5_1.htm`. Accessed 14 October 2014.

Butterfield, R. and Banerjee, P. (1971). The elastic analysis of compressible piles and pile groups. *Geotechnique*, 21(1):43–60.

Chow, L. (1994). *The prediction of surface settlements due to tunnelling in soft ground*. PhD thesis, Brasenose College, University of Oxford.

Das, B. M. and Sobhan, K. (2010). *Principles of Geotechnical Engineering, SI*. Cengage Learning, Stamford, USA, 8th edition.

Dominguez, B. (1966). Stress and displacements in semi-infinite media. Master's thesis, Universidad Nacional de Bueonos Aires.

Douglas, D. J. and Davis, E. H. (1964). The movement of buried footings due to moment and horizontal load and the movement of anchor plates. *Geotechnique*, 14(2):115–132.

Dwight, H. B. (1957). *Tables of integrals and other mathematical data*. The Macmillan Company, New York, 3rd edition.

Geddes, J. D. (1966). Stresses in foundation soils due to vertical subsurface loading. *Geotechnique*, 16(3).

Geddes, J. D. (1969). Boussinesq-based approximations to the vertical stresses caused by pile-type subsurface loadings. *Geotechnique*, 19(4):509–514.

Mindlin, R. (1936). Force at a point in the interior of a semi-infinite solid. *Physics*, 7(5):195–202.

Neumann, E. (2004). Numerical vs. analytical solutions. `http://www.myphysicslab.com/numerical_vs_analytic.html`. Accessed 7 May 2014.

Perloff, W. H. and Baron, W. (1976). *Soil Mechanics Principles and Applications*. John Wiley Sons.

Poulos, H. and Davis, E. (1974). *Elastic Solutions for Soil and Rock Mechanics*. Centre for Geotechnical Research, University of Sydney.

Powrie, W. (2001). *Soil Mechanics Concepts Applications*. Spon Press, 2nd edition.

Rahman, M. and Newaz, G. (2000). Boussinesq type solution for transversely isotropic half-space coated with a thin film. *International Journal of Engineering Science*, 38(7):807–822.

Sabatini, P. J., Pass, D. G., and Bachus, R. C. (1999). *Geotechnical Engineering Circular No.4 - Ground Anchors and Anchored Systems*. GeoSyntec Consultants, 1100 Lake Hearn Drive, Atlanta, Georgia.

Selvadurai, A. P. S. (1979). The displacement of a rigid circular foundation anchored to an isotropic elastic half-space. *Geotechnique*, 29(2):195–202.

Selvadurai, A. P. S. (2001). Mindlin's problem for a halfspace with a bonded flexural surface constraint. *Mechanics Research Communications*, 28(2):157–164.

Sun, H. S., Lei, G. H., Ng, C. W. W., and Zheng, Q. (2013). Displacements under linearly distributed pressures by extended Mindlins equations. *Computers and Geotechnics*, 50:143–149.

Tian-quan, Y. (1981). Pile analysis by simple integral equation methods. *Applied Mathematics and Mechanics*, 2(3).

Timoshenko, S. and Goodier, J. (1951). *Theory of Elasticity*. McGraw-Hill Book Company.

Vaziri, H., Simpson, B., Pappin, J. W., and Simpson, L. (1982). Integrated forms of Mindlin's equations. *Geotechnique*, 32(3):275–278.

Zhang, J. F., Chen, J. J., Wang, J. H., and Zhu, Y. F. (2013). Prediction of tunnel displacement induced by adjacent excavation in soft soil. *Tunnelling and Underground Space Technology*, 36:24–33.

Appendix A

Project Specification

ENG4111/4112

PROJECT SPECIFICATION

FOR: Timothy Eaton

TOPIC: Exploring the application of closed form solutions in geotechnical problems

SUPERVISOR: Dr Kazem Ghabraie

ENROLMENT: ENG4111 – S1, 2014
ENG4112 – S2, 2014

PROJECT AIM: To subject established geotechnical equations towards geotechnical problems with the aim to achieve greater insight in to the relationships of associated elements within them.

PROGRAMME:

1) Research, identify and select a number of related geotechnical equations.

2) Research and identify a number of geotechnical problems in which these equations may be applied.

3) Manipulate, apply mathematical operations and if needed combine equations in order to achieve desired outcomes.

4) Compare and analyse results.

5) Explore the applications of the data.

As time permits:

6) Compare analytical solutions with available numerical solutions.

AGREED T Eaton (student) Date: 17 /03/2014

Ghabraie (supervisor) Date: 17/03/2014

_____ (Examiner/Co-Examiner) Date: /03/2014

Appendix B

General

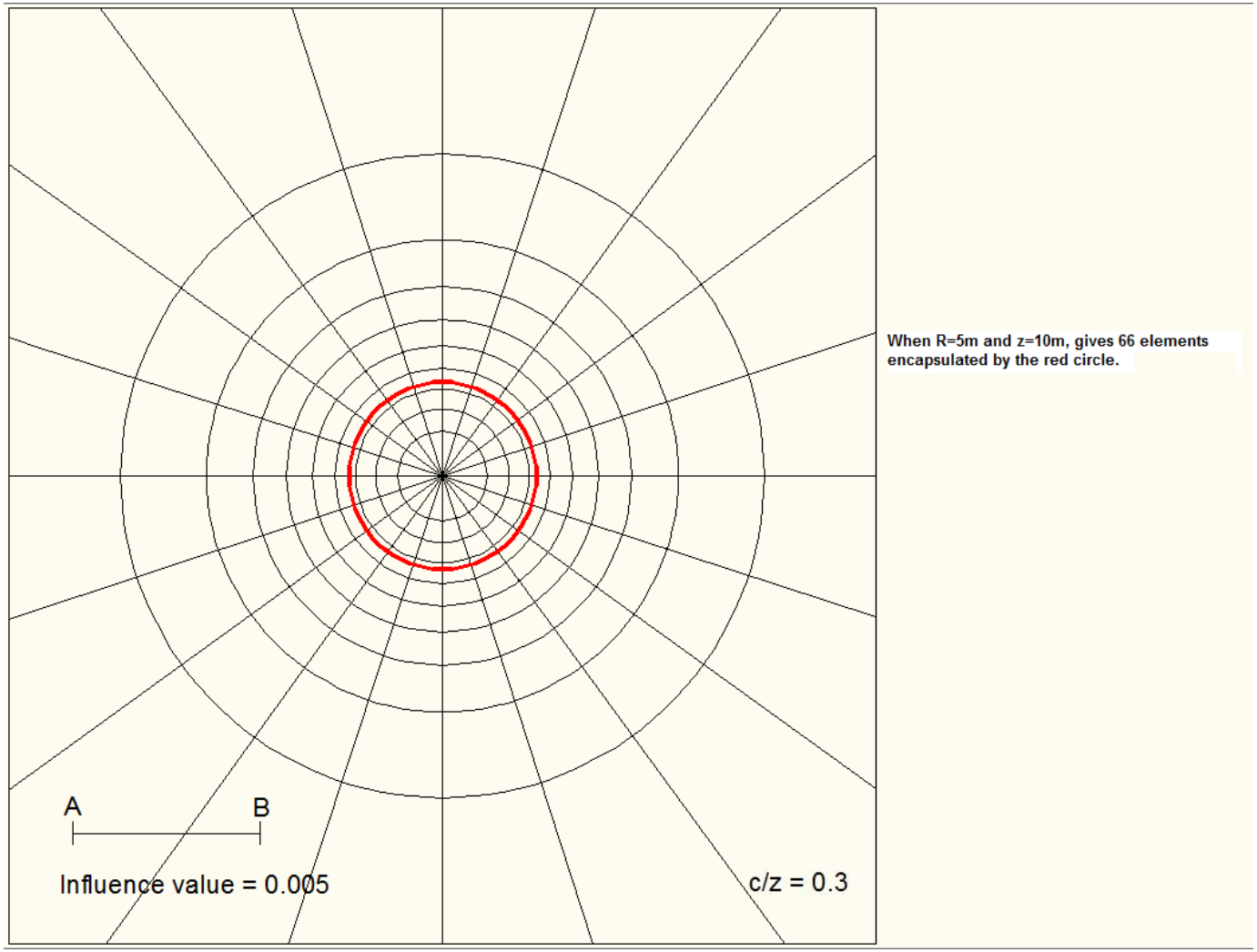

Figure B.1: Mindlin based influence chart for test 1 performed in section 5.1

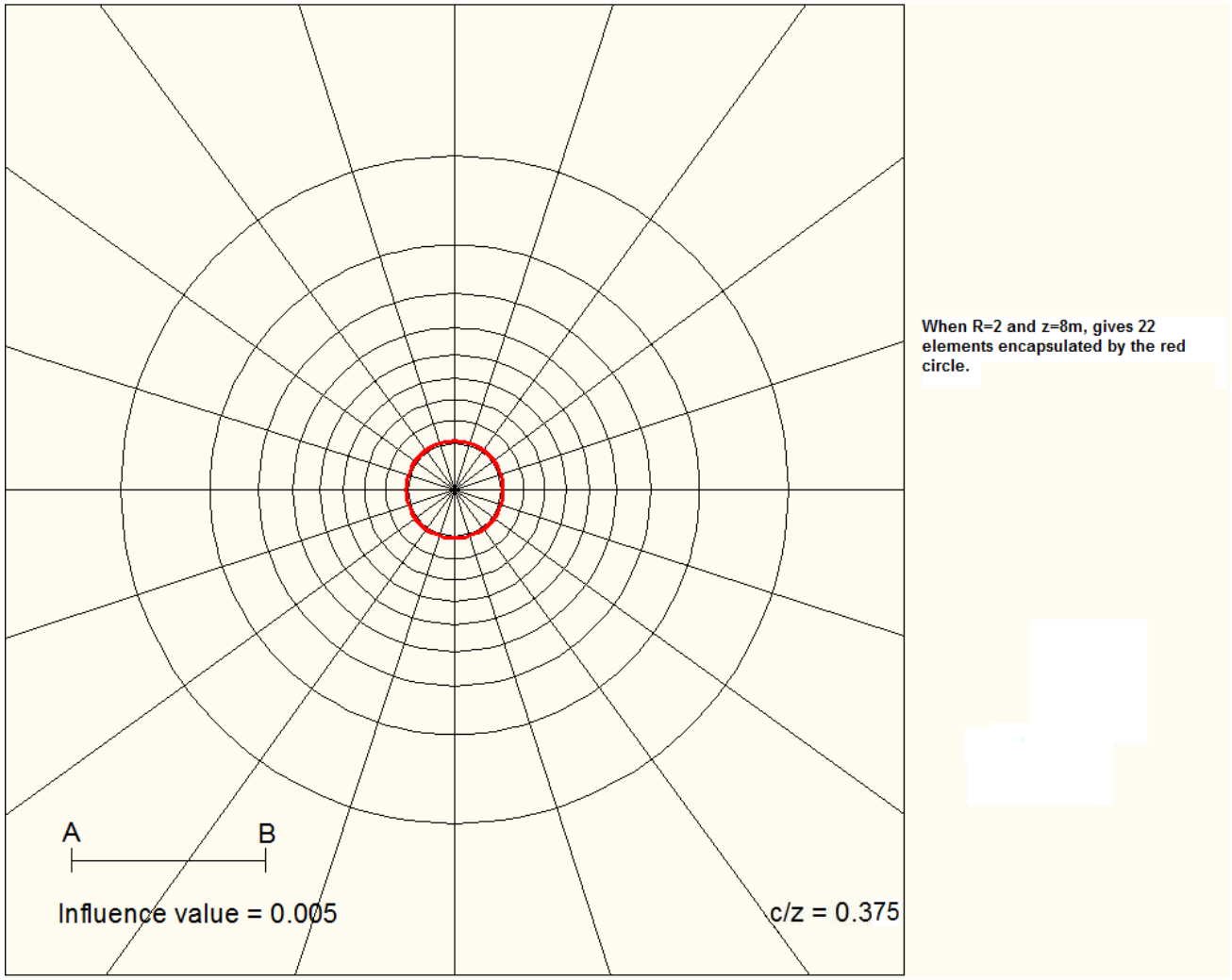

Figure B.2: Mindlin based influence chart for test 2 performed in section 5.1

Appendix C

MATLAB Code

```
function Inffactor = IntegMindlin_F(v,z,c,R)

%Calculating Terms of Equation 4.12 Individually
m = 3*(3-4*v)*z*(z+c).^2 - 3*c*(z+c)*(5*z-c);   %Numerator for terms 7,8
tn = (1-2*v)*(z-c);                             %Numerator for terms 1-4

t1 = tn./[(R.^2+(z-c)^2).^0.5];                 %Term 1
t2 = tn./[((z-c)^2).^0.5];                      %Term 2
t3 = tn./[(R.^2+(z+c)^2).^0.5];                 %Term 3
t4 = tn./[((z+c)^2).^0.5];                      %Term 4
t5 = ((z-c)^3)./[(R.^2+(z-c)^2).^1.5];          %Term 5
t6 = ((z-c)^3)./[((z-c)^2).^1.5];               %Term 6
t7 = m./[3*(R.^2+(z+c)^2).^1.5];                %Term 7
t8 = m./[3*((z+c)^2).^1.5];                     %Term 8
t9 = (6*c*z*(z+c)^3)./(R.^2+(z+c)^2).^2.5;      %Term 9
t10 = (6*c*z*(z+c)^3)./((z+c)^2).^2.5;          %Term 10

Inffactor = -(1./(4-4*v)).*(t1 - t2 - t3 + t4 + t5 - t6 + t7 - t8 + t9
         - t10);
```

```
%ENG4111/4112 Research Project
%Name: Tim Eaton
%File: MindlinPlot_F.m
%For plotting Mindlin-Boussinesq Influence Factor Curves
%Last modified 14th September, 2014
clear all
close all
clc
z = 4;                      %Depth to point of interest (metres)
c = 3.99999;                %Depth to Mindlin loading (metres)
R = 0:0.1:20;               %Radius of circular distributed load (metres)
x = R/z;
for     v = 0:0.1:0.5;              %Poisson's Ratio
        y = IntegMindlin_F(v,z,c,R);

        %Plotting
        hold all
        grid on
        plot(x,y)
        axis([0 5 0.5 1.05])
        xlabel('R/z')
        ylabel('Influence Factor')
        title('Mindlin - Boussinesq Influence Factor Curves z=c');
end

%Calculating and plotting Boussinesq's Equation
B = 1-(z.^3)./[(R.^2+z.^2).^(3/2)];
plot(x,B,'LineWidth',2)
legend('Nu = 0','Nu = 0.1','Nu = 0.2','Nu = 0.3','Nu = 0.4','Nu = 0.5'
       ,'Boussinesq')
```

```
%ENG4111/4112 Research Project
%Name: Tim Eaton
%File: MindlinBoussinesqStresswithDepth.m
%For observing Mindlin - Boussinesq stress behaviour against depth
%Last modified 14th September, 2014
clear all
close all
clc

z = 0:0.001:20;           %Depth to point of interest (metres)
c = 4.00001;              %Depth to Mindlin loading (metres)
R = 1;                    %Radius of circular distributed load (metres)

for     v = 0:0.1:0.5;                        %Poisson's Ratio
        x = IntegMindlin_F(v,z,c,R);

        hold all
        grid on
        plot(x,-z)
        ylabel('z (m)')
        xlabel('Influence Factor')
        title('Mindlin - Boussinesq Influence Factor with Depth');
end

%Calculating and plotting Boussinesq's Equation
        B = 1-(z.^3)./(R.^2+z.^2).^(3/2);
        plot(B,-z,'LineWidth',2)
        legend('Nu = 0','Nu = 0.1','Nu = 0.2','Nu = 0.3','Nu = 0.4'
              ,'Nu = 0.5','Boussinesq')
```

```
%ENG4111/4112 Research Project
%Name: Tim Eaton
%File: CombinedPlot.m
%For observing Mindlin - Boussinesq COMBINED stress behaviour against depth
%Last modified 14th September, 2014
clear all
close all
clc

z = 0:0.001:20;          %Depth to point of interest (metres)
c = 3.99999;             %Depth to Mindlin loading (metres)
R = 4;                   %Radius of circular distributed load (metres)

%Calculating Boussinesq's Equation
%1.233 obtained from script file MindlinPlot_F.m
B = 1-(z.^3)./((1.233*R)^2+z.^2).^(3/2);

for     v = 0.5;                          %Poisson's Ratio
        x = IntegMindlin_F(v,z,c,R) + B;

        hold all
        grid on
        plot(x,-z)
        ylabel('z (m)')
        xlabel('Influence Factor')
        title('Combined Mindlin - Boussinesq Influence Factor with Depth');
        legend('Nu = 0.5')
end
```

```
%ENG4111/4112 Research Project
%Name: Tim Eaton
%File: qb.m
%For finding max ratio of qB/qM that is required to nullify all tensile
%stresses
%Last modified 14th September, 2014
clear all
close all
clc

z = 0:0.001:20;     %Depth to point of interest (metres)
c = 3.99999;        %Depth to Mindlin loading (metres)
R = 4;              %Radius of circular distributed loads (metres)(RB=RM)
B = 1-(z.^3)./((R).^2+z.^2).^(3/2);

for v = 0.5;                                        %Poisson's Ratio
    Q = (IntegMindlin_F(v,z,c,R))./-B;              %Ratio of qB/qM

    hold all
    grid on
    plot(Q,-z)
    xlabel('q_B/q_M')
    ylabel('z(m)')
    title('Load Ratio required for Zero Tensile Stresses against Depth
          , R/c = 1');
    legend('Nu = 0.5')
end
```

```
%ENG4111/4112 Research Project
%Name: Tim Eaton
%File: ModifiedIF.m
%For checking ratio obtained from script qb.m
%Last modified 14th September, 2014
clear all
close all
clc

z = 0:0.001:20;       %Depth to point of interest (metres)
c = 3.99999;          %Depth to Mindlin loading (metres)
R = 4;                %Radius of circular distributed load (metres)
Q = 1.593;            %qB/qM ratio obtained from script qb.m plot

%Calculating Boussinesq's Equation
B = 1-(z.^3)./((R)^2+z.^2).^(3/2);

for     v = 0.5;                              %Poisson's Ratio
        y = IntegMindlin_F(v,z,c,R) + Q*B;

        hold all
        grid on
        plot(y,-z)
        xlabel('Modified Influence Factor')
        ylabel('z(m)')
        title('Modified Influence Factor with Depth');
        legend('Nu = 0.5')
end
```

```
%ENG4111/4112 Research Project
%Name: Tim Eaton
%File: nosurcharge.m
%For seeing at what depth Mindlin stresses are canceled out by self weight
%of soil
%Last modified 18th September, 2014
clear all
close all
clc

z = 0:0.001:20;              %Depth to point of interest (metres)
c = 7.00001;                 %Depth to Mindlin loading (metres)
R = 2;                       %Radius of circular distributed load (metres)
q = 300;                     %Mindlin load kPa
gamma = 18;                  %Unit weight of the soil kN/m^3
G = gamma.*z;                %Stress due to soil weight kPa

for     v = 0:0.1:0.5;       %Poisson's Ratio
        x = IntegMindlin_F(v,z,c,R).*q + G;

        hold all
        grid on
        plot(x,-z)
        ylabel('z (m)')
        xlabel('Stress (kPa)')
        title('Mindlin vs soil weight with Depth');
        legend('Nu = 0','Nu = 0.1','Nu = 0.2','Nu = 0.3','Nu = 0.4'
               ,'Nu = 0.5')
end
```

```
%ENG4111/4112 Research Project
%Name: Tim Eaton
%File: qratio_max_plot.m
%For finding max values of qB/qM that is required to nullify all tensile
%stresses for each value of R/c
%Last modified 12th October, 2014
clear all
close all
clc

Z = 0:0.001:20;       %Depth to point of interest (metres)
C = 1.99999;          %Depth to Mindlin loading (metres)
z = Z./C;             %dimensionless transformation
c = 1;                %dimensionless transformation
%r = Radius of circular distribute loads (metres)(RB=RM)
%v = Poisson's ratio
%Q = Ratio of qB/qM

%%%%%%CASE 1%%%%%%
i=0;
v = 0.5;
for r = 0.00001:0.1:10.00001;
    R = r./C;
    i = i+1;
    A(i) = r./C;
    B = 1-(Z.^3)./((r).^2+Z.^2).^(3/2);
    Q = (IntegMindlin_F(v,z,c,R))./-B;
    qmax(i) = max(Q);

    hold all
```

```
    grid on
    plot(A,qmax)
    axis([0 5 1 6])
    ylabel('Ratio of q_B to q_M')
    xlabel('R/c')
    title('Required ratio q_B/q_M to nullify all Tensile Stresses')
end

%%%%%%CASE 2%%%%%%
v=0.4;
for r = 0.00001:0.1:10.00001;
    R = r./C;
    i = i+1;
    A4(i) = r./C;
    B = 1-(Z.^3)./((r).^2+Z.^2).^(3/2);
    Q = (IntegMindlin_F(v,z,c,R))./-B;
    qmax4(i) = max(Q);

    plot(A4,qmax4)
end

%%%%%%CASE 3%%%%%%
v=0.3;
for r = 0.00001:0.1:10.00001;
    R = r./C;
    i = i+1;
    A3(i) = r./C;
    B = 1-(Z.^3)./((r).^2+Z.^2).^(3/2);
    Q = (IntegMindlin_F(v,z,c,R))./-B;
    qmax3(i) = max(Q);
```

```
    plot(A3,qmax3)
end

%%%%%%CASE 4%%%%%%
v=0.2;
for r = 0.00001:0.1:10.00001;
    R = r./C;
    i = i+1;
    A2(i) = r./C;
    B = 1-(Z.^3)./((r).^2+Z.^2).^(3/2);
    Q = (IntegMindlin_F(v,z,c,R))./-B;
    qmax2(i) = max(Q);

    plot(A2,qmax2)
end

%%%%%%CASE 5%%%%%%
v=0.1;
for r = 0.00001:0.1:10.00001;
    R = r./C;
    i = i+1;
    A1(i) = r./C;
    B = 1-(Z.^3)./((r).^2+Z.^2).^(3/2);
    Q = (IntegMindlin_F(v,z,c,R))./-B;
    qmax1(i) = max(Q);

    plot(A1,qmax1)
    legend('v = 0.1','v = 0.2','v = 0.3','v = 0.4','v = 0.5')
end
```